MSCs can be a useful source of cells for transplantation for several reasons: they have the ability to proliferate and differentiate into mesodermal tissues, including heart, they entail no ethical or immunological problems, and bone marrow aspiration is an established routine procedure. When placed in appropriate *in vitro* and *in vivo* environments, MSCs can give rise to all major mesenchymal tissues, such as bone, cartilage, muscle, and adipose tissue [18]. Murine MSCs can also differentiate into cardiomyocytes and start to beat synchronously *in vitro* [19], and direct injection of murine MSCs into the heart has been shown to be feasible in murine models of ischemic heart disease and normal mouse heart. Thus far, only endothelial cells have been shown to exhibit '*in vitro* cardiomyogenesis' in humans [20].

Large numbers of cells must be injected into damaged sites in ischemic heart disease to restore cardiac function in humans, and cells need to be injected into the entire heart in cardiomyopathy. Until now, however, there have been no reports of a sufficient number of differentiated human cardiomyocytes ever having been obtained to restore the function of a failing heart. One of the reasons for this is that the life span of human cells *in vitro* is limited. Human cells reach senescence or stop cell growth after a limited number of cell replications [21], and the average number of hMSC population doublings (PDs) has been found to be 38 [22], implying that it would be difficult to obtain enough cells to restore the function of a failing human heart.

To resolve these problems and to establish a model of cell therapy of the failing heart, we attempted to prolong the life span of hMSCs by using the system to infect retrovirus encoding bmi-1, human telomerase reverse transcriptase (TERT), and human papillomavirus E6 and E7 genes. Both Rb/p16INK4a inactivation with E7 and telomerase activation with E6 are required to extend the life span of human epithelial cells [23]. bmi-1, a c-myc cooperating oncogene in murine lymphomas, reduces expression of p16INK4a, stimulates cell proliferation [24], and is required for maintenance of self-renewing hematopoietic stem cells [25,26]. This method was highly efficient in extending the life span of hMSCs. In the present study we investigated whether hMSCs with an extended life span have the ability to differentiate into cardiomyocytes *in vitro*.

Materials and methods

Isolation and cell culture of hMSCs

After obtaining signed informed consent, bone marrow cells were harvested from a 91-year-old human female donor with the approval of the Ethics Committee of Keio University School of Medicine (Tokyo). Cells were resuspended in bone marrow stromal cell culture medium (10% fetal bovine serum in Dulbecco's modified Eagle's medium containing 4.5 g/l glucose [DMEM-HG]) with antibiotic/antimycotic supplements (Gibco), and cultures were maintained at 37 °C in a humidified atmosphere containing 95% air and 5% CO_2. When the cultures reached subconfluence, the cells were harvested with 0.25% trypsin and 1 mM EDTA, and replated with one half of the harvested cells. After a series of passages, the attached marrow stromal cells were devoid of hematopoietic cells. Several bone marrow stromal cell strains were then generated by the limiting-dilution method, and one of them was designated H4-1. The H4-1 cells were cultured in MSC growth medium (MSCGM) at 37 °C in a humidified atmosphere containing 95% air and 5% CO_2.

Preparation and infection of recombinant retroviruses

The full-length human bmi-1 cDNA was cloned by RT-PCR using RNA extracted from K562 cells. Thermoscript reverse transcriptase (Invitrogen) and KOD polymerase (TOYOBO, Japan) were used for the RT and PCR reactions, respectively. The forward primer, 5′-ACGCGTCGACCGCCATGCATCGAACAACGAGAAT-3′, and reverse primer, 5′-CGGATCCTCAACCAGAAGAAGTTGCTG-3′, were designed to obtain the coding sequence of human bmi-1 flanked by the *Sal*I site (underlined) and the Kozak consensus sequence at the 5′-end and the *Bam*HI site (underlined) at the 3′-end. The *Sal*I-*Bam*HI segment of the PCR product was cloned between the *Xho*I and *Bgl*II sites of pCLXSN to generate pCLXSN-bmi1. The coding sequence of the cDNA was confirmed to be identical to the published sequence (NCBI ACC# NM_005 180.4). Construction of pCLXSH-hTERT has been described previously [27]. The gateway system (Invitrogen) was used to subclone a deletion mutant of HPV16 E6 (16E6SDD151) that lacked transforming activity to 3Y1 cells [28] into pCMSCVpuro. pCMSCVpuro comprises the CMV/LTR fusion promoter, the packaging signal Psi, and the multicloning sequence from pCLXSN (Imgenex Corp., San Diego, CA, USA) followed by the PGK-puro cassette and the 3′ long terminal repeat of murine embryonic stem cell virus from pMSCVpuro (Clontech). The destination vector pCMSCVpuro-DEST was constructed by inserting a modified cassette containing attR sites and ccdB (Invitrogen) between the *Eco*RI and *Bgl*II sites of pCMSCVpuro. 16E6SDD151 was first recombined into pDONR201 by BP reaction, and then into the destination vector by LR reaction according to the manufacturer's instructions (Invitrogen) to generate pCMSCVpuro-16E6SDD151. Production of recombinant retroviruses has been described previously [29,30]. Briefly, the retroviral vector together with the packaging construct, pCL-10A1, was transfected into 293T cells, and the culture fluid was harvested 48–72 h post-transfection. The preparation of the LXSN-16E7 retrovirus and the infection protocols have been described previously [31], except that FLYA13 [32] was used as the packaging cell line instead of PG13. The titers of the recombinant viruses were greater than 5×10^5 drug-resistant colony-forming units per milliliter on HeLa

cells, and 1 ml of the culture fluid was added to the cells in the presence of polybrene (8 μg/ml). Following inoculation with the viruses, hMSCs were grown in the presence of G418 (100 μg/ml), hygromycin B (50 μg/ml), or puromycin (1 μg/ml), and a polyclonal drug-resistant cell line was established and further analyzed. To achieve combinations of retroviral infections, cells were sequentially transduced with LXSN-E7 or LXSN-bmi-1, and LXSH-hTERT, and then MSCVpuro-16E6SDD151, if indicated, and selected with G418, hygromycin B, and puromycin, respectively. The stably transduced cells with an expanded life span were designated UBT-5, UBET-7, UEET-1, UEET-11, and UET-13.

Flow cytometric analysis

Cells were detached and stained for 30 min at 4 °C with primary antibodies and immunofluorescent secondary antibodies. After washing, the cells were analyzed on an EPICS ALTRA analyzer (Beckman Coulter). Antibodies (anti-human CD13, CD14, CD24, CD29, CD31, CD34, CD44, CD45, CD50, CD54, CD55, CD59, CD90, CD105, CD117, CD133, CD140a, CD166, Flk-1) were purchased from Beckman Coulter, Immunotech, Cytotech, and Pharmingen Pharmaceutical, Inc.

Introduction of the GFP and β-galactosidase genes

Recombinant adenovirus expressing β-galactosidase and the green fluorescent protein (GFP) was prepared as described [33]. Cells were infected with these viruses at 10 plaque-forming units/cell. hMSCs were examined cytochemically *in vitro* for expression of the β-galactosidase gene and by fluorescent confocal microscopy for expression of the GFP gene. By 7 days post-infection nearly all the cells expressed β-galactosidase and GFP.

Preparation of murine fetal cardiomyocytes

Fetal cardiomyocytes were obtained from the hearts of day 14 mouse fetuses. Hearts were minced with scissors and washed with phosphate-buffered saline (PBS), and the minced hearts were incubated in PBS with 0.05% trypsin and 0.25 mM EDTA for 5 min at 37 °C. After adding DMEM supplemented with 10% fetal bovine serum (FBS), the cardiomyocytes were centrifuged at 1000 rpm for 5 min. The pellet was then resuspended in 10 ml DMEM with 10% FBS and incubated on glass dishes for 1 h to separate the cardiomyocytes from fibroblasts. The floating cardiomyocytes were collected and replated at $1 \times 10^5/cm^2$.

hMSC and murine fetal cardiomyocyte co-culture system

Human MSCs were plated on dishes at $5 \times 10^4/cm^2$, and infected with EGFP-expressing adenovirus on the next day. The supernatant was then removed, and the cells were cultured for 2 days in DMEM supplemented with 10% FBS. The cells were then exposed to 10 μM of 5-azacytidine for 24 h to induce cell differentiation. The 5-azacytidine-treated hMSCs were harvested with 0.25% trypsin and 1 mM EDTA and overlaid onto the fetal cardiomyocytes at $5 \times 10^3/cm^2$. The morphology of the beating hMSCs was evaluated under a fluorescent microscope.

RT-PCR

Total RNA was prepared from co-cultured hMSCs and mouse heart with Isogen (Nippon Gene). Human cardiac RNA was purchased (Clontech). RNA for RT-PCR was converted to cDNA with a first-strand cDNA synthesis kit (Amersham Pharmacia Biotec) according to the manufacturer's recommendations. RT-PCR of the bmi-1, E6, E7, TERT, myosin light chain-2a (MLC-2a), Nkx2.5, and human atrial natriuretic peptide (hANP) genes was performed, and the PCR primers used are listed in Table 1. RT-PCR was performed with PCR primers that can amplify human but not mouse genes. PCR primers of 18S used as a positive control react with both human and murine genes. PCR was performed with TaKaRa Z-Taq (Takara Shuzo Co., Ltd) for 30 cycles, with each cycle consisting of 98 °C for 5 s, 68 °C or 60 °C for 1 s, and 72 °C for 10 s, with an additional 30-s incubation at 72 °C after completion of the final cycle.

Action potential recording and microinjection of dye

An inverted microscope (IX-70, Olympus, Tokyo, Japan) with a fluorescence filter (U-MNIBA2, Olympus) was used for action potential (AP) recording. The microscope was equipped with a recording chamber and a noise-free heating plate (Microwarm Plate, Kitazato Supply, Fujinomiya, Shizuoka, Japan). A 10 mmol/l volume of HEPES was added to the culture medium to stabilize the pH of the perfusate at 7.5–7.6. Standard glass microelectrodes having a DC resistance of 25–35 MΩ when filled with pipette solution were used. Alexa 568 compound was dissolved to a concentration of 0.5 mmol/l in 2 mol/l of KCl solution in order to completely dissolve the Alexa 568 in the pipette solution. The electrodes were positioned with a motor-driven micromanipulator (PCS-5000, Burleigh Instruments, Inc., New York, USA) under optical control. Spontaneously beating GFP-positive cells were selected as targets, and, after the APs of the targeted cells had been recorded, the dye was injected by iontophoresis (−7 nA for 30–60 s). The extent

Table 1. PCR primers used in this study

Gene product	Primer (sense)	Primer (anti-sense)	Annealing temperature (°C)	Product size (bp)
Bmi-1	TCATCCTTCTGCTGATGCTG	GCATCACAGTCATTGCTGCT	60	220
E6	GACCCAGAAAGTTACCACAG	GCAACAAGACATACATCGAC	60	397
E7	ATGACAGCTCAGAGGAGGAG	TCCTAGTGTGCCCATTAACAG	60	178
TERT	CGGAAGAGTGTCTGGAGCAA	GGATGAAGCGGAGTCTGGA	60	144
MLC-2a				
1st	TCGTGATGGCATCATCTGCAAGG	ACAGAGTTTATTGAGGTGCCCC	60	429
2nd	AAGGTGAGTGTCCCAGAGG	ATGGGTGTCAGGGCGAACATC	60	259
NkX2.5				
1st	CTTCAAGCCAGAGGCCTACG	CCGCCTCTGTCTTCTCCAGC	60	233
2nd	CTTCACCGGCCAAGTGTGCGTC	CCGCCTCTGTCTTCTCCAGC	60	152
hANP				
1st	GAACCAGAGGGGAGAGACAGAG	CCCTCAGCTTGCTTTTTAGGAG	60	406
2nd	GTCAGACCAGAGCTAATCCC	ACCTCCATCTCTCTGGGCTG	68	223
18S	GTGGAGCGATTTGTCTGGTT	CGCTGAGCCAGTCAGTGTAG	60	200

of dye transfer was monitored under a fluorescence microscope, and digital images were recorded with a digital photo camera (D100; Nikon, Tokyo, Japan) mounted on the microscope with a fluorescence filter (U-MWIG2; Olympus). The recording pipette was connected to a patch-clamp amplifier (Axopatch 200B; Axon Instruments), and the signal was low-pass filtered at 2 kHz and digitized with an A/D converter with sampling frequency of 10 kHz (Digidata 1322A; Axon Instruments) connected to a computer with Pentium4. Signals were monitored, recorded as electric files, and analyzed offline with pCLAMP 8.2 software (Axon Instruments). The rhythm was considered regular if the maximum beating rate minus the minimum beating rate divided by the max beating rate was <0.4.

Immunohistochemistry

The hMSCs co-cultured with fetal cardiomyocytes *in vitro* were fixed with 4% PFA and stained with anti-β2microglobulin antibody at 1 : 1000, mouse monoclonal antibody against troponin I (Hytest, Euro, Finland) at 1 : 200, anti-desmin antibody at 1 : 100, and anti-β-galactosidase antibody (Chemicon) at 1 : 500. hMSCs expressing GFP were fixed with 4% PFA.

Results

Establishment of hMSCs with an extended life span

H4-1 cells were obtained from primary culture by limiting dilution (Figure 1A). The cells proliferated for a limited number of passages and then underwent senescence, as evidenced by the cells assuming a broad and flattened shape (Figures 1B and 1C). To extend the life span of H4-1 cells, and obtain a large number of cells for cardiac transplantation, four different types of cells were obtained by transferring combinations of bmi-1, E6, E7, and/or TERT genes. Cells transduced with bmi-1 and TERT were designated UBT-5 cells; cells transduced with bmi-1, E6, and TERT were named UBET-7 cells; cells transduced with E7 and TERT were designated UET-13 cells; and cells transduced with E6, E7, and TERT were named UEET-1 and UEET-11 cells (Figures 1D, 1E, and 1F). To simplify nomenclature and avoid confusion, we use the name UEET-1 to refer to cells transduced with E6, E7, and TERT although they have recently been reported as ThMSC1 [29]. The cells were subcloned after each gene transfer, and thus were clonal. The UEET-1 cells were spindle-shaped, and longer than the parental H4-1 cells (Figures 1B, 1D, and 1E). Characteristics of cells with a prolonged life span were investigated. UEET-11 and UET-13 proliferated more than 150 PDs in 400 days, and UBET-7 and UBT-5 proliferated more than 50 PDs in 400 days, while H4-1 stopped dividing at 38 PDs (approximately 200 days). The growth rates of UEET-11 and UET-13 were higher than those of UBT-5 and UBET-7. Chromosome analysis revealed parental H4-1 and UET-13 to exhibit normal karyotypes, while the other cells transduced with E6 and E7 showed chromosome aberrations at low frequencies (data not shown). The transduced cells did not generate tumors, at least for the first 60 days after subcutaneous transplantation into immunodeficient mice.

Surface analysis of hMSCs

Surface markers of the UEET-1, UEET-11, UBT-5, UBET-7, and UET-13 cells were evaluated by flow cytometric analysis. The results showed that all of the MSCs were positive for CD13, CD29 (integrin β1), CD44 (Pgp-1/ly-24), CD55, CD59, CD90 (Thy-1), CD105 (endoglin), CD133, CD140a (PDGFRα or PDGFR2), and CD166 (ALCAM), and negative for CD14 (a marker for macrophage and dendritic cells), CD24, CD31 (PECAM-1), CD34, CD45 (leukocyte common antigen), CD50 (ICAM-3), CD54, CD117 (c-kit), and Flk-1 (Figure 2). Parental H4-1 cells had the same pattern of surface markers as UEET-1, UEET-11, UBT-5, and UBET-7 cells, implying that the surface markers were not influenced by

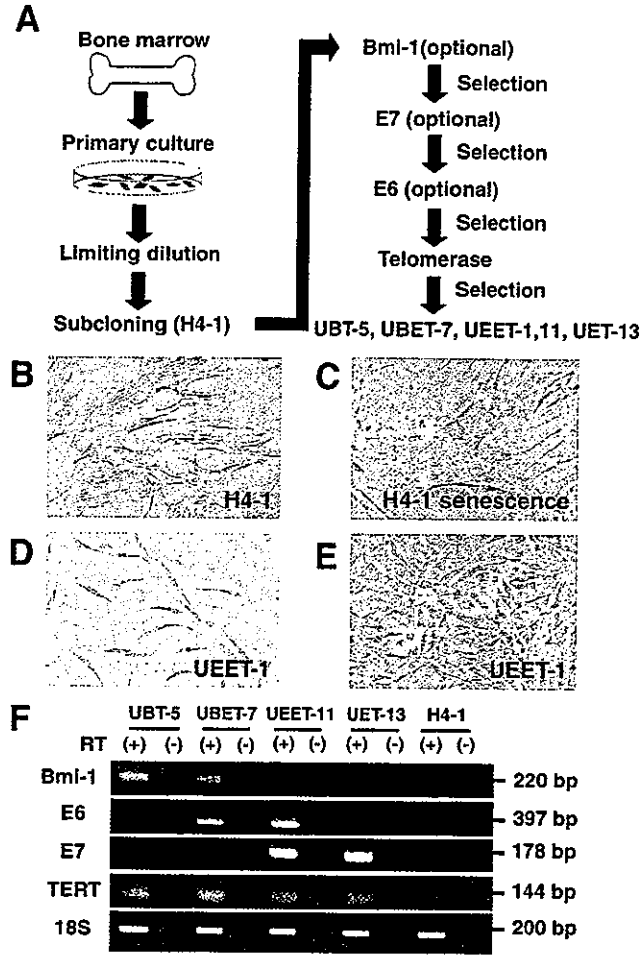

Figure 1. Experimental scheme. (A) Bone marrow stromal cells were obtained from a human donor and subcloned by limiting dilution. One of the cells isolated was designated H4-1 cells, and they were transduced with E6, E7, TERT, or bmi-1 genes to extend their life span. The combinations of genes transferred were: (1) bmi-1 and TERT; (2) bmi-1, E7, and TERT; (3) E7 and TERT; and (4) E6, E7, and TERT. (B) H4-1 cells in the growth phase. (C) H4-1 cells at senescence. The cells showed a broad and flattened shape. (D) H4-1 cells after transfer of E6, E7, and TERT genes were designated UEET-1 cells. (E) UEET-1 cells at confluence. Original magnification, B–E: ×100. (F) The gene expression in each cell line was analyzed using RT-PCR

the exogeneously expressed bmi-1, E6, E7, and/or TERT genes.

Cardiomyogenic differentiation of hMSCs and stably transduced hMSCs

To determine whether H4-1 cells could be induced to undergo cardiomyogenic differentiation, the cells were exposed to 10 μM of 5-azacytidine for 24 h as previously reported in murine stromal cells [19]. All of the transduced hMSCs did not exhibit spontaneous beating despite continuous culturing for up to 3 months. Immunocytochemical analysis revealed the presence of desmin, a myocytic marker, in the hMSCs with an extended life span, i.e., UBT-5 cells and UBET-7 cells (Figure 3A). However, all cells tested were negative for the cardiomyocyte marker troponin-I (Figure 3B).

We employed a co-culture system with fetal cardiomyocytes to induce cardiac differentiation (Figure 4), since *in vitro* simulation of the heart by the environment has been shown to be an efficient means of induced differentiation of human endothelial progenitor cells and murine marrow stromal cells [20,34]. After exposing GFP-labeled UBT-5, UBET-7, UEET-11, and UET-13 cells to 10 μM of 5-azacytidine for 24 h, these cells were co-cultured with fetal cardiomyocytes. On day 3 after the start of co-cultivation, a few GFP-positive UBET-7 cells started to contract (Figure 5A). The contraction was stronger when beating cells were clustered than when scattered (Figure 5B). On day 7, the beating of the UBET-7 cells was synchronous with that of adjacent cells and was independent of that of the surrounding murine cardiomyocytes (Figures 5C and 5D). Repetition of these experiments confirmed the results to be reproducible, and the percentages of UBT-5, UBET-7, UEET-11, and UET-13 cells that underwent cardiomyogenic differentiation were almost the same, implying that cardiomyogenic differentiation is independent of the genes transferred. The number of beating cells increased for up to 3–4 weeks, when the fetal cardiomyocytes spontaneously detached from the dishes (Figure 5E). UBET-7 cells not treated with 5-azacytidine were co-cultured with fetal cardiomyocytes to determine whether environmental factors alone can induce cardiac differentiation, but fewer beating cells were observed (Figure 5F). No significant difference was detected in the number of differentiated cells between parental H4-1 and UBET-7 (Figure 5G).

Expression of cardiomyocyte-specific genes and proteins and the action potential of differentiated hMSCs

We analyzed the co-cultured UBET-7 cells in terms of gene expression and by immunocytochemistry and electrical recording. RT-PCR was performed with primers that react with human cardiomyocyte-specific genes but not with murine orthologues. Differentiated UBET-7 cells expressed MLC-2a, hANP, and the cardiomyocyte-specific transcription factor, Nkx2.5/Csx (Figure 6). Sequence analysis revealed that the cDNAs matched the sequences of the human MLC-2a, hANP, and Nkx2.5/Csx genes.

Action potentials were recorded from spontaneously beating cells. Alexa 568 was injected into cells via a recording microelectrode to stain the cells and confirm that the action potential was generated by GFP-positive UBET-7 cells (Figures 7A and 7B). Since the dye did not diffuse into the murine cardiomyocytes, there were no tight cell-to-cell heterologous connections, i.e., gap junctions. In some experiments, Alexa 568 diffused into the GFP-positive satellite UBET-7 cells, suggesting that a homologous cell-to-cell connection had been established at least 1 week after co-cultivation. The measured parameters of the recorded action potential were averaged

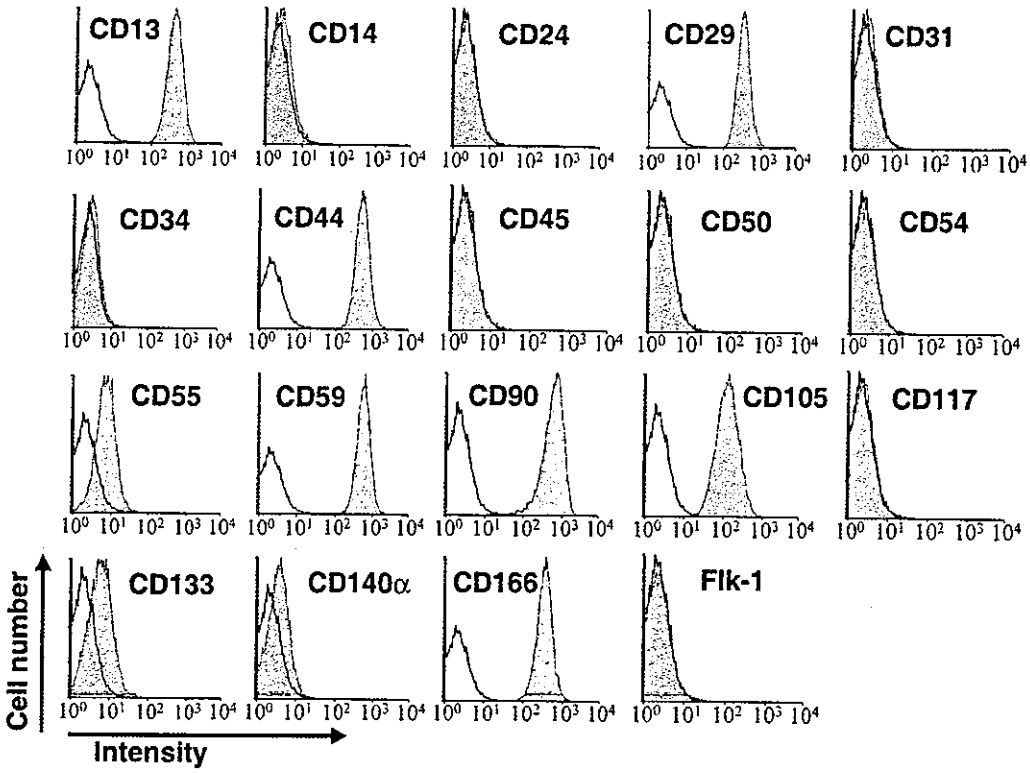

Figure 2. Flow cytometric analysis of UEET-1 cells. UEET-1 cells were labeled with FITC-coupled antibodies against CD13, CD14, CD24, CD29, CD31, CD34, CD44, CD45, CD50, CD54, CD55, CD59, CD90, CD105, CD117, CD133, CD140a, CD166, and Flk-1 and analyzed with an EPICS ALTRA analyzer

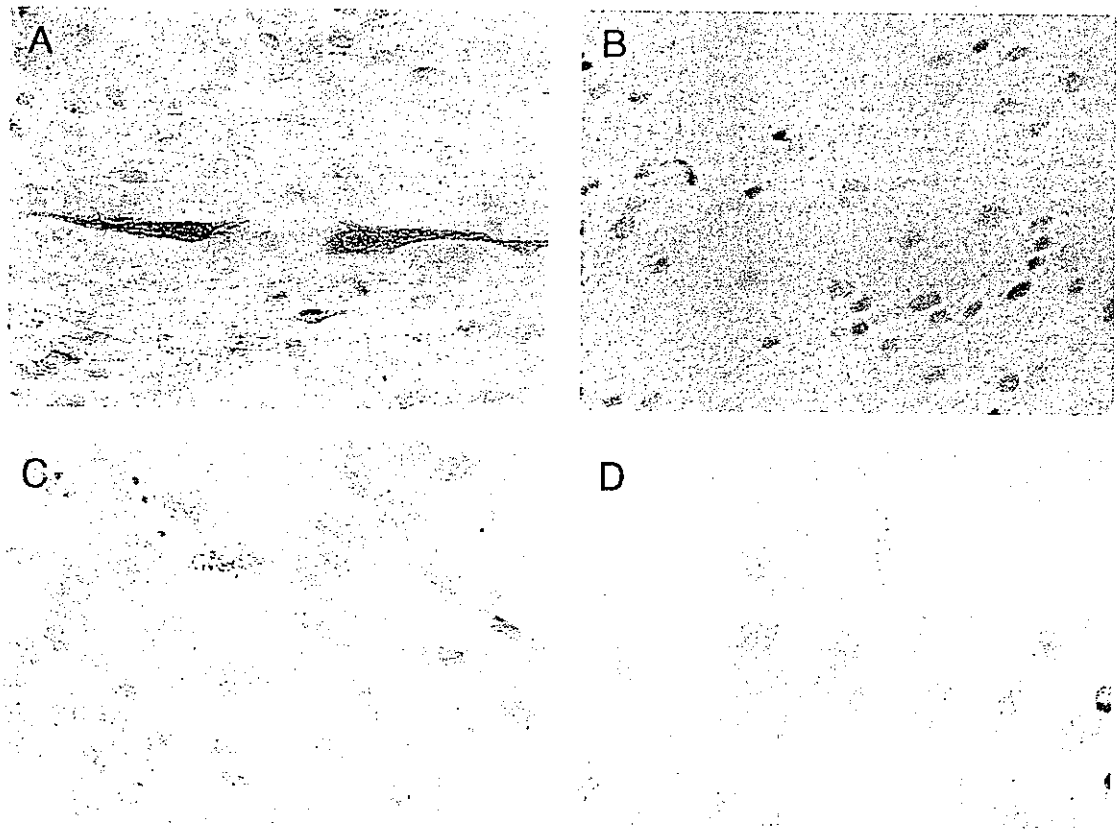

Figure 3. Immunostaining of hMSCs with anti-desmin and anti-troponin-I antibodies after exposure to 5-azacytidine. UBET-7 cells were exposed to 10 μM of 5-azacytidine for 24 h and stained for desmin (A) and cardiac troponin I (B). UBET-7 cells not treated with 5-azacytidine were also stained for desmin (C) and cardiac troponin I (D). Original magnification: ×400

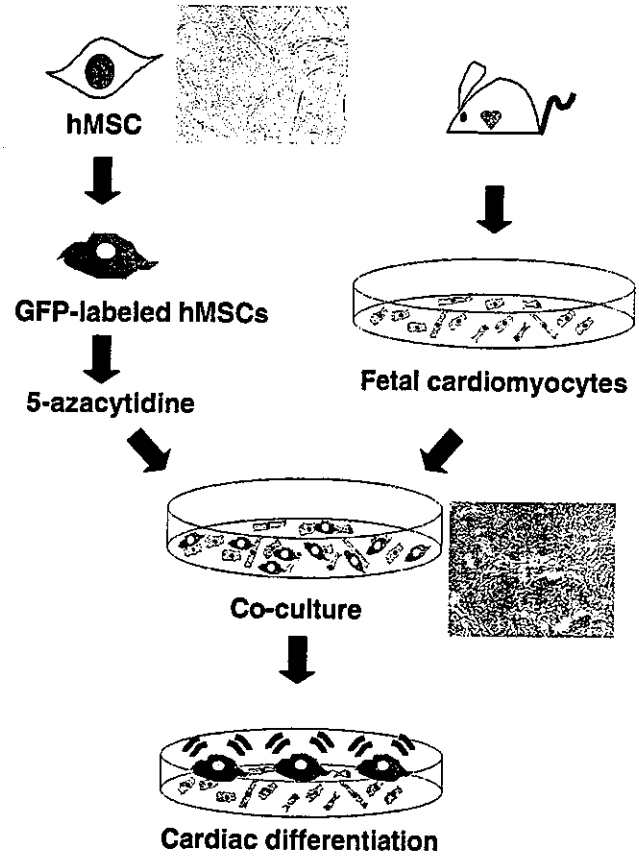

Figure 4. Scheme of the co-culture system. hMSCs infected with adenoviruses carrying the GFP gene were treated with 10 μM of 5-azacytidine for 24 h. hMSCs expressing GFP were then co-cultured with murine fetal cardiomyocytes. hMSCs began beating spontaneously after 7 days of co-culture

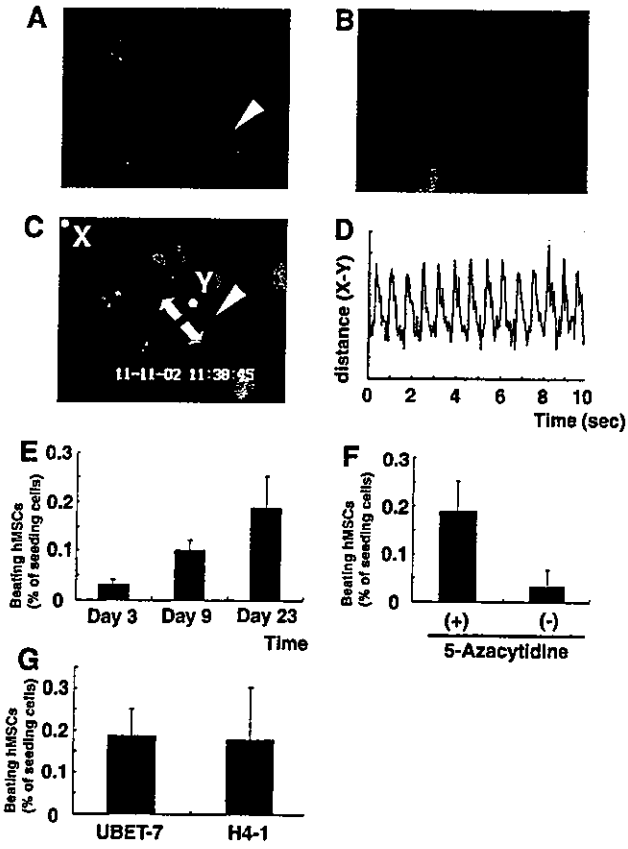

Figure 5. Beating of hMSCs in the *in vitro* co-culture system. (A) 5-Azacytidine-treated GFP-positive UBET-7 cells were co-cultured with murine fetal cardiomyocytes (http://1985.jukuin.keio.ac.jp/umeza/jgm/ubet7). The white arrowhead is pointing to some beating UBET-7 cells whose rhythm was different from that of the fetal cardiomyocytes. (B) More UBET-7 cells tended to contract in areas where they were clustered than in areas where they were scattered. (C) Beating UBET-7 cells were videotaped at 30 flames/s and their contractions were analyzed. Point X in this view was fixed, and point Y was used as a reference point on the differentiated UBET-7 cell (arrowhead). Arrows point in the direction of contraction, and point Y moved with each contraction. Original magnification, A–C: ×150. (D) The distances between points X and Y were measured for a 10-s period and plotted on the graph. The UBET-7 cells contracted regularly at 84 beats/min. (E) The ratio of the number of beating UBET-7 cells to the number of the cells seeded increased for 3 weeks. (F) On day 23, the ratio was higher in the cells exposed to 5-azacytidine than in the cells not exposed to 5-azacytidine. (G) Parental H4-1 was compared with UBET-7 in terms of the number of beating cells

(Table 2). The duration of the action potentials of the UBET-7 cells was extremely long, and they were therefore concluded to be action potentials of cardiomyocytes, not of smooth muscle, nerve cells, or skeletal muscle. Time-course analysis of the action potentials revealed shortening of their duration, a gain in amplitude, and stabilization and organization of the spontaneous beating rhythm. Representative action potential recordings are shown in Figures 7C and 7D. The rhythm of some (33%) of the UBET-7 cells was still disorganized at 1 week (Figure 7C), whereas the rhythm of the UBET-7 cells (100%) had become regular and had stabilized at 3 weeks (Figure 7D).

Immunohistochemistry revealed that UBET-7 cells expressing human β2microglobulin and GFP stained positive for desmin (Figures 8A–8C) and cardiac troponin I (Figures 8D–8F) on day 14. Clear striations were observed in the differentiated UBET-7 cells (Figure 8H).

Absence of cell fusion between hMSCs and murine fetal cardiomyocytes

To determine whether the beating cells had fused with the fetal cardiomyocytes, GFP-expressing hMSCs were co-cultured with fetal cardiomyocytes labeled with β-galactosidase. On day 7, when almost 100% of the cardiomyocytes were labeled with β-galactosidase, and almost 100% of the co-cultured-hMSCs expressed GFP, none of the cells were double-stained for GFP and β-galactosidase (Figures 9A–9D). This observation indicates that the cardiomyogenic differentiation of hMSCs is not attributable to cell fusion on day 7.

Discussion

This study was conducted to determine whether prolongation of cell life span by cell-cycle-associated molecules

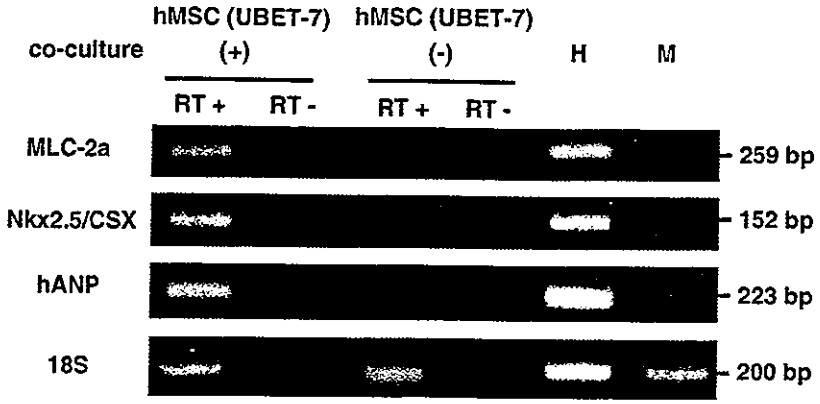

Figure 6. Expression of cardiomyocyte-specific genes in differentiated hMSCs (UBET-7). RT-PCR was performed with PCR primers that react with human genes encoding cardiac proteins (MLC-2a, Nkx2.5, and hANP) but do not with the murine genes. Only the 18S PCR primer used as a positive control reacted with the human and murine genes. Human heart (H) and mouse heart (M) were used as a positive control and negative control, respectively. The human cardiac genes, MLC-2a, Nkx2.5/csx and hANP, were expressed in the co-culturing system, but were not expressed in the undifferentiated state (without feeder cells)

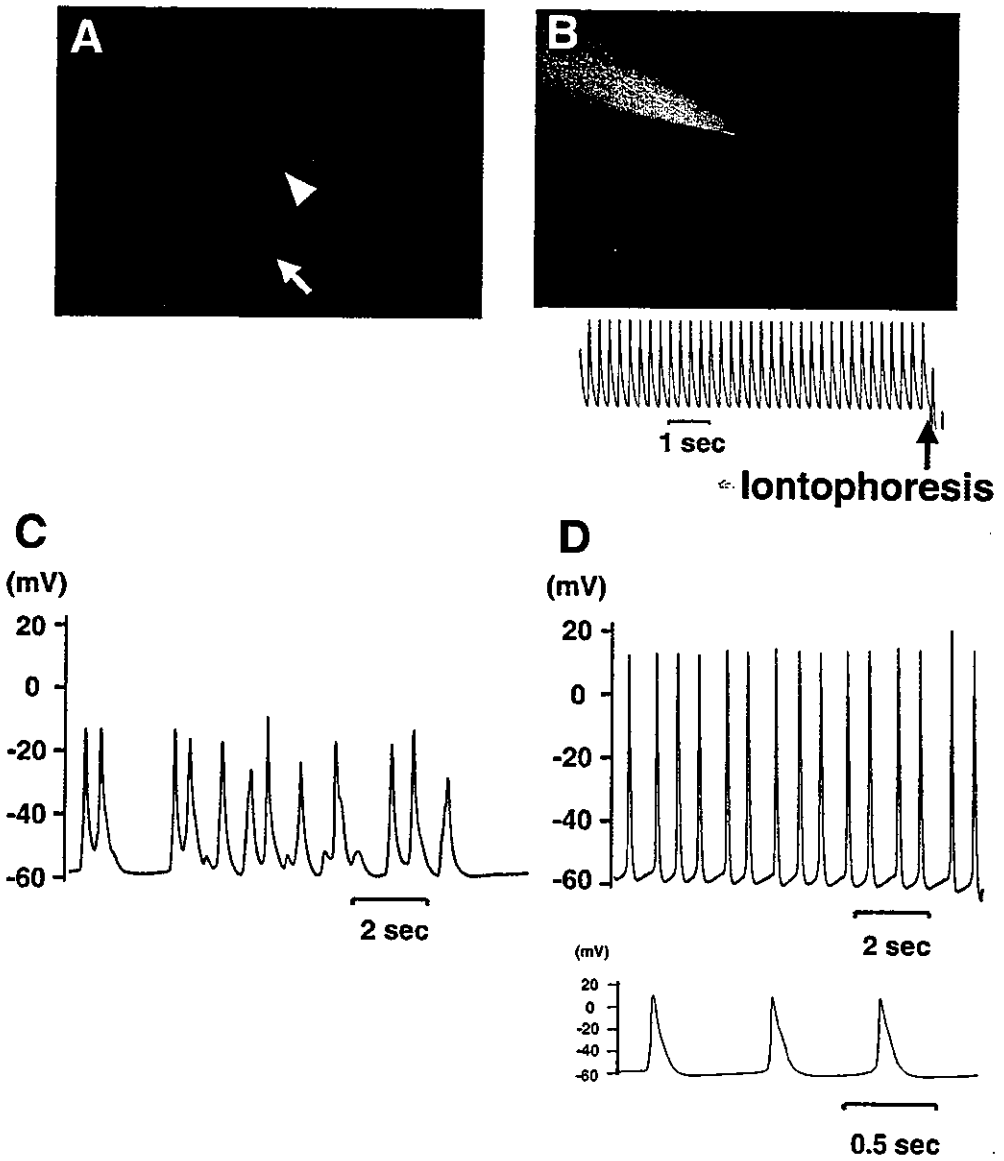

Figure 7. Action potentials of beating hMSCs. GFP-labeled UBET-7 cells (A) were injected with Alexa 568 solution (B) by iontophoresis through a microelectrode. The injected UBET-7 cell and neighboring beating UBET-7 cell are indicated by arrowhead and arrow, respectively. The action potential was recorded (B, lower panel). Some of the rhythms recorded at 1 week of co-cultivation were irregular (C), but the rhythm became regular at 3 weeks (D); top: large scale (2 s), bottom: small scale (0.5 s). Original magnification, A, B: ×400

Table 2. Action potential parameters in human mesenchymal stem cell derived cardiomyocytes

Time of co-culture	n	Ratio of regular rate	Beating rate (beats/min)	MDP (mV)	Amplitude (mV)	APD_{90} (ms)
1 week	12	67%	70.6 ± 12.8	−49.9 ± 1.6	47.2 ± 2.9	345.8 ± 21.4
2 weeks	9	67%	65.9 ± 12.7	−50.3 ± 2.3	60.2 ± 4.5	169.7 ± 13.8
3 weeks	9	100%	68.2 ± 12.1	−45.1 ± 1.4	63.7 ± 3.0	163.4 ± 16.5

The values are shown as mean ± S.E. The ratio of regular rate: regular beating rhythm/irregular beating rhythm. MDP: maximum diastolic potential. APD: action potential duration.

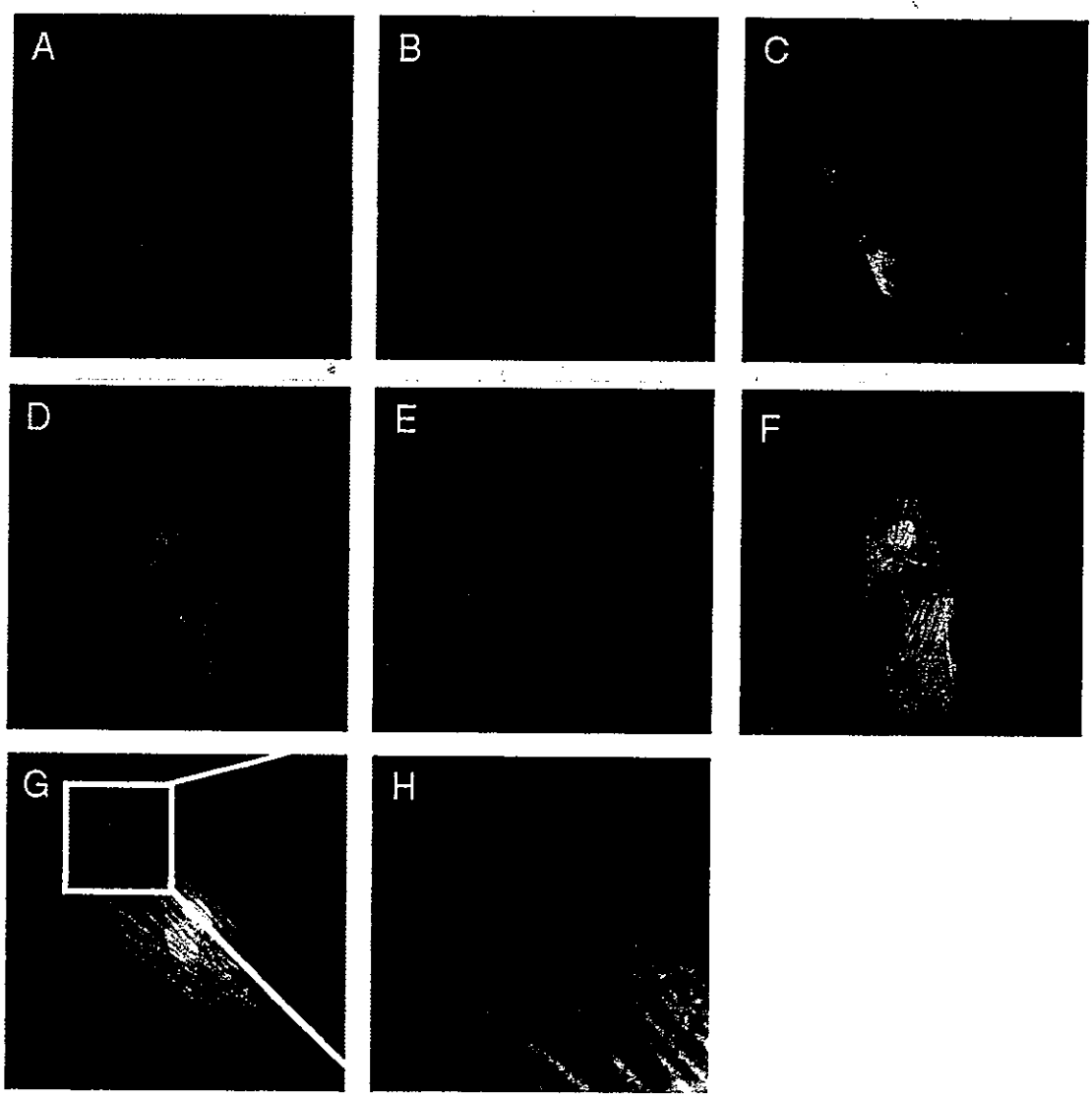

Figure 8. Immunocytochemistry of differentiated hMSCs with anti-desmin and anti-troponin-I antibodies. UBET-7 cells were co-cultured with cardiomyocytes. UBET-7 cells were analyzed for myogenic and cardiac differentiation by immunohistochemistry with desmin and cardiac troponin-I, respectively. Co-cultured UBET-7 cells were stained with anti-β2microglobulin antibody (A) and anti-desmin antibody (B). A superimposed image ('Merge') of A and B is shown in C. GFP-expressing UBET-7 cells (D) were stained with anti-troponin-I antibody (E). 'Merge' is shown in F. A differentiated UBET-7 cell is shown at higher magnification (G). The differentiated UBET-7 cells have striations in their cytoplasm (H). Original magnification, A–G: ×600, H: ×2000

would predominate over cardiomyogenic differentiation of marrow stromal cells *in vitro*. The primary findings of the present study were: (1) the life span of hMSCs was extended by bmi-1, E6, E7, and TERT; (2) hMSCs exposed to 5-azacytidine and cultured with fetal cardiomyocytes underwent cardiomyogenic differentiation as manifested by their morphology, gene expression, and electrophysiology, and started to beat spontaneously (automaticity); and (3) cardiomyogenic differentiation of the hMSCs was not attributable to cell fusion.

MSCs are pluripotent cells capable of differentiating into many cell types, such as neurons [35], myocytes, cardiomyocytes, chondrocytes, and adipocytes [36]. Multipotent adult progenitor cells (MAPCs) have recently

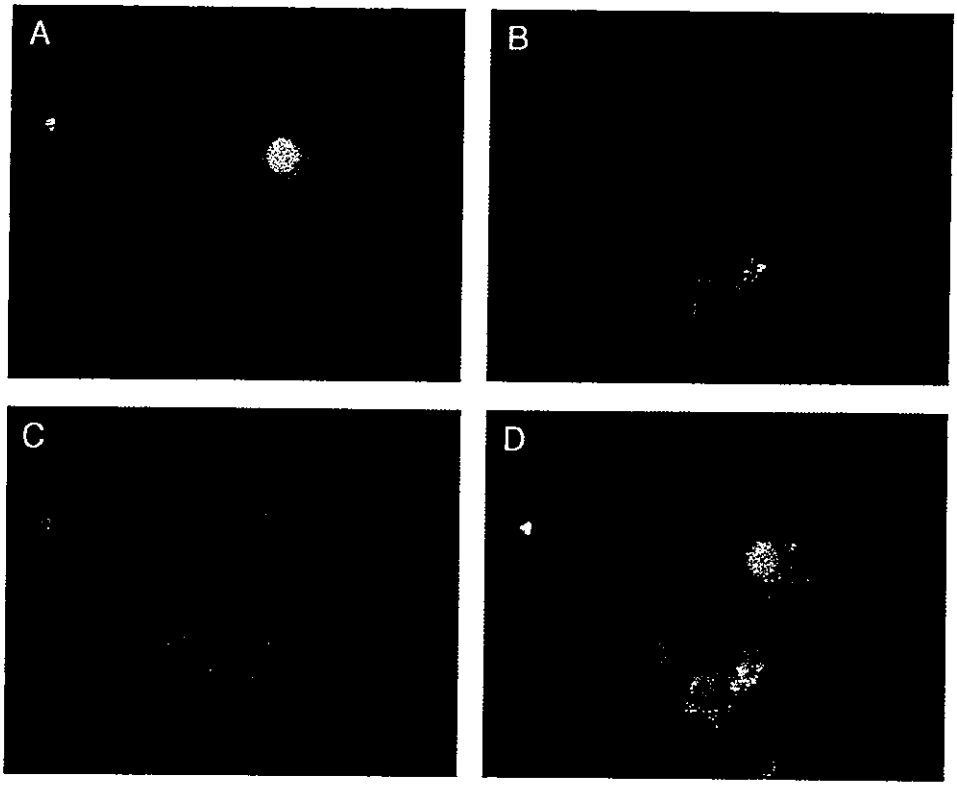

Figure 9. Cardiomyogenic differentiation of hMSCs is not due to cell fusion. We labeled UBET-7 cells with GFP (A) and murine cardiomyocytes with β-galactosidase (B). Cells were tested for the presence of β-galactosidase immunocytochemically (B, Cy5). Differentiation of UBET-7 cells was determined with anti-troponin I antibody (C, Rhodamine). 'Merge' of A, B, and C is shown in D. The differentiated GFP-expressing UBET-7 cells had not fused with murine feeder cells labeled with β-galactosidase. Original magnification: ×600

been shown to differentiate, at single cell level, not only into mesenchymal cells, but also into cells with characteristics of visceral mesoderm, neuroectoderm, and endoderm [37]. MAPCs have the ability to proliferate extensively without any clear evidence of senescence or loss of differentiation potential, and they are thought to be extremely similar to embryonic stem (ES) cells. MSCs and MAPCs also have the advantages of the absence of ethical and immunological problems, and undesired differentiation is infrequent. Thus they are one of the most promising sources of cells for cell therapy.

However, there are two major problems with hMSCs: (1) a large enough number of cells to regenerate tissue by cell transplantation is difficult to obtain, and (2) detailed investigation has been limited by their finite life span. A system that allows human cells to escape senescence by using cell-cycle-associated molecules may be used to obtain sources of cell therapy and to overcome these problems and establish a good model of cell transplantation to the failing heart [23,38]. Both inactivation of the Rb/p16INK4a pathway and activation of telomerase are required for immortalization of human epithelial cells such as mammary epithelial cells and skin keratinocytes. Human papillomavirus E7 can inactivate pRb, and bmi-1 can repress p16INK4a expression. Inactivation of the p53 pathway is also beneficial, even if not essential, to extension of the life span [39]. Based on the above notion, we transferred E7 or bmi-1 plus hTERT in combination with or without E6 into hMSCs and obtained several hMSC strains with an extended life span: UEET-1, UBT-5, UBET-7, UEET-11, and UET-13 cells. The cells with the extended life span continued growing *in vitro* for over 150 PDs, and their differentiation potential was maintained. Transfer of TERT alone was insufficient to prolong the life span of hMSCs in the present study, despite TERT having been reported to extend the life span of cells beyond senescence without affecting their differentiation ability [40]. The characteristics of the cells with an extended life span were unchanged after transfer of bmi-1, E6, E7, and TERT genes, and this finding is consistent with flow cytometric analysis showing that the surface markers of H4-1 cells and stably transduced cells (UEET-1, UBT-5, UBET-7, UEET-11, and UET-13) are identical [29].

In this study, we used the demethylating agent 5-azacytidine as an inducer, the same as in murine marrow stromal cells [19], and clearly showed that co-cultivation with fetal cardiomyocytes is necessary to induce cardiomyogenic differentiation which could be further enhanced by pretreatment of cells with 5-azacytidine. 5-Azacytidine is a cytosine analog that has a remarkable effect on transdifferentiation of cells and has been shown to induce differentiation of mesenchymal cells into cardiomyocytes, skeletal myocytes, adipocytes, and chondrocytes [19,41]. The effect of this low-molecular substance is not surprising, since 5-azacytidine

is incorporated into DNA and has been shown to cause extensive demethylation. The demethylation is attributable to covalent binding of DNA methyltransferase to 5-azacytidine in the DNA [42], with the subsequent reduction of enzyme activity in cells resulting in dilution-out and random loss of methylation at many sites in the genome. This may in turn account for the reactivation of cardiomyogenic 'master' genes, such as MEF-2C, GATA4, dHAND, and Nkx2.5/Csx, leading to stochastic transdifferentiation of MSCs into cardiomyocytes. Use of 5-azacytidine is beneficial, but since it may have drawbacks, i.e., gene activation leading to oncogenesis and undesired differentiation, care must be exercised before using it to simply induce cells to differentiate into target phenotype(s) because of its stochastic nature.

Thus, it may be necessary to find alternative humoral factors essential for cardiomyogenic differentiation to prepare cells for cell therapy in humans. In addition to demethylating agents, environmental factors promote cardiomyocyte differentiation. A co-culture system has recently been used to induce cardiac differentiation, and human endothelial progenitor cells have been found to transdifferentiate into cardiomyocytes with this system [20]. Murine MSCs have been shown to differentiate into a cardiomyogenic lineage [43], but to our knowledge the present study is the first to report spontaneous beating by human MSCs and exhibition of *'in vitro'* automaticity without cell fusion. These results simply imply that MSCs may have the ability to transdifferentiate into cardiomyocytes in response to demethylation of the genome, in addition to environmental factors.

Co-cultivation makes it difficult to investigate two different types of cells in detail because they are present on the same dishes, and the target cells are difficult to isolate. There was also the question of whether the presence of beating cells means differentiation to cardiomyocytes, or merely fusion with fetal cardiomyocytes. Since marrow cells spontaneously fuse with co-cultured ES cells *in vitro* [44], controversy has arisen as to whether regenerated myocardium represents transplanted cells fused with native cardiomyocytes instead of differentiated donor cells. Cell fusion did not occur in our study, however, because cardiomyogenic differentiation was demonstrated by the double-labeling of two types of co-cultured cells *in vitro*.

The co-culture of the target cells, i.e., the marrow stroma, in this study, on appropriate feeder cells may provide a good system for generating a source of cells for therapy. hMSCs have the ability to form tight cell-to-cell couplings, i.e., gap junctions, with adjacent hMSCs, suggesting that the grafted hMSCs are capable of generating electrical coupling and may function coordinately in the recipient human heart. On the other hand, the disorganization of the spontaneous beating rhythm in the early stage may result in arrhythmogenesis when grafted into the recipient. Early afterdepolarization, which triggers arrhythmias, has been reported in cardiomyocytes generated by ES cells or embryonal carcinoma cells [45]. By contrast, the absence of early afterdepolarization in hMSCs may be beneficial in terms of not leading to arrhythmias when the cells are transplanted *in vivo*. The rhythm of the hMSCs that underwent premature differentiation became regular after complete differentiation in the present study, and culture for a certain period therefore seems necessary before cell transplantation. It is noteworthy that the risk of lethal arrhythmia can be reduced by promoting electrical maturation of hMSCs *in vitro* when this co-culture system is used for therapy clinically.

It remains unresolved how co-cultured hMSCs start beating spontaneously and what the key factor(s) in cardiac differentiation are. Several factors promote differentiation into cardiomyocytes, such as gap junctions, humoral factors, electrical and mechanical stimulation, and cell-to-cell contact. Gap junctions have been shown to be necessary for differentiation of endothelial progenitor cells to cardiomyocytes [20], but the lack of gap junctional communication between hMSCs and feeder cells in our study indicates that gap junctions are not prerequisite for differentiation. In addition, separation of hMSCs and fetal cardiomyocytes in a co-culture system with a membrane that is permeable to humoral factors but not to cells resulted in loss of capacity for cardiac differentiation (data not shown), implying that humoral factors alone do not induce cardiac differentiation of hMSCs, and direct interactions, such as with cell-membrane bound molecules and extracellular matrix, seem to be essential. Cadherins, for example, have been reported to mediate calcium-dependent cell-to-cell contact and affect the differentiation of cardiac muscle cells [46]. Moreover, the decrease in number of beating hMSCs after the feeder cells stopped beating implies that mechanical stimulation in addition to cell-to-cell contact might be indispensable to cardiac differentiation and maintenance of the differentiated state.

Many clinical trials of regeneration therapy using mononuclear cells for the failing heart have been performed [13–16], but many more basic studies are needed. hMSCs with an expanded life span cannot be transplanted clinically, because they have been transduced with human papillomavirus E6 and E7 genes. The present results and others have shown that these molecules do not elicit cell transformation *in vitro*, at least during the period observed. This contrasts with human stromal cells being transformed during immortalization by SV40 large T antigen [47]. Based on the results of this study and the mechanism of cell life span extension, we are now developing a novel strategy to eliminate the possibility of transformation. Thus, cells that undergo reproducible cardiomyogenic differentiation and have a prolonged life span can be used as a good model of cell transplantation.

Acknowledgements

We would like to express our sincere thanks to K. Tsuchiya, T. Uyama and S. Matsumoto for support throughout the work, and T. Inomata, Y. Nakamura, and Y. Taki for providing expert

technical assistance. We are grateful to Dr. D. A. Galloway (FHCRC, Seattle, USA) for pLXSN-16E7 and to Dr. Y. Takeuchi (Chester Beatty Laboratories, ICR, UK) for the FLYA13 cells. This work was supported in part by a special grant for Advanced Research on Cancer from the Ministry of Education, Culture, Sports, Science, and Technology of Japan to T. K. and A. U., and the Organization for Pharmaceutical Safety and Research to A.U.

The cell names are summarized at http://1985.jukuin.keio.ac.jp/umezawa/cells/name.html. MPEG video stream of UBET-7 is available at http://1985.jukuin.keio.ac.jp/umezawa/jgm/ubet7.

References

1. Klug MG, Soonpaa MH, Koh GY, Field LJ. Genetically selected cardiomyocytes from differentiating embryonic stem cells form stable intracardiac grafts. *J Clin Invest* 1996; **98**: 216–224.
2. Min JY, Yang Y, Converso KL, *et al.* Transplantation of embryonic stem cells improves cardiac function in postinfarcted rats. *J Appl Physiol* 2002; **92**: 288–296.
3. Etzion S, Battler A, Barbash IM, *et al.* Influence of embryonic cardiomyocyte transplantation on the progression of heart failure in a rat model of extensive myocardial infarction. *J Mol Cell Cardiol* 2001; **33**: 1321–1330.
4. Muller-Ehmsen J, Whittaker P, Kloner RA, *et al.* Survival and development of neonatal rat cardiomyocytes transplanted into adult myocardium. *J Mol Cell Cardiol* 2002; **34**: 107–116.
5. Muller-Ehmsen J, Peterson KL, Kedes L, *et al.* Rebuilding a damaged heart: long-term survival of transplanted neonatal rat cardiomyocytes after myocardial infarction and effect on cardiac function. *Circulation* 2002; **105**: 1720–1726.
6. Ghostine S, Carrion C, Souza LC, *et al.* Long-term efficacy of myoblast transplantation on regional structure and function after myocardial infarction. *Circulation* 2002; **106**: I131–136.
7. Taylor DA, Atkins BZ, Hungspreugs P, *et al.* Regenerating functional myocardium: improved performance after skeletal myoblast transplantation. *Nat Med* 1998; **4**: 929–933.
8. Jackson KA, Majka SM, Wang H, *et al.* Regeneration of ischemic cardiac muscle and vascular endothelium by adult stem cells. *J Clin Invest* 2001; **107**: 1395–1402.
9. Orlic D, Kajstura J, Chimenti S, *et al.* Bone marrow cells regenerate infarcted myocardium. *Nature* 2001; **410**: 701–705.
10. Wang JS, Shum-Tim D, Galipeau J, Chedrawy E, Eliopoulos N, Chiu RC. Marrow stromal cells for cellular cardiomyoplasty: feasibility and potential clinical advantages. *J Thorac Cardiovasc Surg* 2000; **120**: 999–1005.
11. Shake JG, Gruber PJ, Baumgartner WA, *et al.* Mesenchymal stem cell implantation in a swine myocardial infarct model: engraftment and functional effects. *Ann Thorac Surg* 2002; **73**: 1919–1925; discussion 1926.
12. Gojo S, Gojo N, Takeda Y, *et al.* In vivo cardiovasculogenesis by direct injection of isolated adult mesenchymal stem cells. *Exp Cell Res* 2003; **288**: 51–59.
13. Strauer BE, Brehm M, Zeus T, *et al.* Repair of infarcted myocardium by autologous intracoronary mononuclear bone marrow cell transplantation in humans. *Circulation* 2002; **106**: 1913–1918.
14. Hamano K, Nishida M, Hirata K, *et al.* Local implantation of autologous bone marrow cells for therapeutic angiogenesis in patients with ischemic heart disease: clinical trial and preliminary results. *Jpn Circ J* 2001; **65**: 845–847.
15. Assmus B, Schachinger V, Teupe C, *et al.* Transplantation of progenitor cells and regeneration enhancement in acute myocardial infarction (TOPCARE-AMI). *Circulation* 2002; **106**: 3009–3017.
16. Tse HF, Kwong YL, Chan JK, Lo G, Ho CL, Lau CP. Angiogenesis in ischaemic myocardium by intramyocardial autologous bone marrow mononuclear cell implantation. *Lancet* 2003; **361**: 47–49.
17. Menasche P, Hagege AA, Scorsin M, *et al.* Myoblast transplantation for heart failure. *Lancet* 2001; **357**: 279–280.
18. Prockop DJ. Marrow stromal cells as stem cells for nonhematopoietic tissues. *Science* 1997; **276**: 71–74.
19. Makino S, Fukuda K, Miyoshi S, *et al.* Cardiomyocytes can be generated from marrow stromal cells in vitro. *J Clin Invest* 1999; **103**: 697–705.
20. Badorff C, Brandes RP, Popp R, *et al.* Transdifferentiation of blood-derived human adult endothelial progenitor cells into functionally active cardiomyocytes. *Circulation* 2003; **107**: 1024–1032.
21. Hayflick L, Moorhead PS. The serial cultivation of human diploid cell strains. *Exp Cell Res* 1961; **25**: 585–621.
22. Bruder SP, Jaiswal N, Haynesworth SE. Growth kinetics, self-renewal, and the osteogenic potential of purified human mesenchymal stem cells during extensive subcultivation and following cryopreservation. *J Cell Biochem* 1997; **64**: 278–294.
23. Kiyono T, Foster SA, Koop JI, McDougall JK, Galloway DA, Klingelhutz AJ. Both Rb/p16INK4a inactivation and telomerase activity are required to immortalize human epithelial cells. *Nature* 1998; **396**: 84–88.
24. Jacobs JJ, Kieboom K, Marino S, DePinho RA, van Lohuizen M. The oncogene and Polycomb-group gene bmi-1 regulates cell proliferation and senescence through the ink4a locus. *Nature* 1999; **397**: 164–168.
25. Lessard J, Sauvageau G. Bmi-1 determines the proliferative capacity of normal and leukaemic stem cells. *Nature* 2003; **423**: 255–260.
26. Park IK, Qian D, Kiel M, *et al.* Bmi-1 is required for maintenance of adult self-renewing haematopoietic stem cells. *Nature* 2003; **423**: 302–305.
27. Okamoto T, Aoyama T, Nakayama T, *et al.* Clonal heterogeneity in differentiation potential of immortalized human mesenchymal stem cells. *Biochem Biophys Res Commun* 2002; **295**: 354–361.
28. Kiyono T, Hiraiwa A, Fujita M, Hayashi Y, Akiyama T, Ishibashi M. Binding of high-risk human papillomavirus E6 oncoproteins to the human homologue of the Drosophila discs large tumor suppressor protein. *Proc Natl Acad Sci U S A* 1997; **94**: 11 612–11 616.
29. Imabayashi H, Mori T, Gojo S, *et al.* Redifferentiation of dedifferentiated chondrocytes and chondrogenesis of human bone marrow stromal cells via chondrosphere formation with expression profiling by large-scale cDNA analysis. *Exp Cell Res* 2003; **288**: 35–50.
30. Naviaux RK, Costanzi E, Haas M, Verma IM. The pCL vector system: rapid production of helper-free, high-titer, recombinant retroviruses. *J Virol* 1996; **70**: 5701–5705.
31. Halbert CL, DG Galloway DA. The E7 gene of human papillomavirus type 16 is sufficient for immortalization of human epithelial cells. *J Virol* 1991; **65**: 473–478.
32. Cosset F-LTY, Battini J-L, Weiss RA, Collins MKL. High-titer packaging cells producing recombinant retroviruses resistant to human serum. *J Virol* 1995; **69**: 7430–7436.
33. Yamashita T, Tonoki H, Nakata D, Yamano S, Segawa K, Moriuchi T. Adenovirus type 5 E1A immortalizes primary rat cells expressing wild-type p53. *Microbiol Immunol* 1999; **43**: 1037–1044.
34. Tomita S, Nakatani T, Fukuhara S, Morisaki T, Yutani C, Kitamura S. Bone marrow stromal cells contract synchronously with cardiomyocytes in a co-culture system. *Jpn J Thorac Cardiovasc Surg* 2002; **50**: 321–324.
35. Kohyama J, Abe H, Shimazaki T, *et al.* Brain from bone: efficient "meta-differentiation" of marrow stroma-derived mature osteoblasts to neurons with Noggin or a demethylating agent. *Differentiation* 2001; **68**: 235–244.
36. Pittenger MF, Mackay AM, Beck SC, *et al.* Multilineage potential of adult human mesenchymal stem cells. *Science* 1999; **284**: 143–147.
37. Jiang Y, Jahagirdar BN, Reinhardt RL, *et al.* Pluripotency of mesenchymal stem cells derived from adult marrow. *Nature* 2002; **418**: 41–49.
38. Romanov SR, Kozakiewicz BK, Holst CR, Stampfer MR, Haupt LM, Tlsty TD. Normal human mammary epithelial cells spontaneously escape senescence and acquire genomic changes. *Nature* 2001; **409**: 633–637.
39. Rheinwald JG, Hahn WC, Ramsey MR, *et al.* A two-stage, p16(INK4A)- and p53-dependent keratinocyte senescence mechanism that limits replicative potential independent of telomere status. *Mol Cell Biol* 2002; **22**: 5157–5172.

40. Bodnar AG, Ouellette M, Frolkis M, *et al.* Extension of life-span by introduction of telomerase into normal human cells. *Science* 1998; **279**: 349–352.
41. Taylor S, Jones PA. Multiple new phenotypes induced in 10T1/2 cells and 3T3 cells treated with 5-azacytidine. *Cell* 1979; **17**: 771–779.
42. Santi DV, Norment A, Garrett CE. Covalent bond formation between a DNA-cytosine methyl transferase and DNA containing 5-azacytidine. *Proc Natl Acad Sci U S A* 1984; **81**: 6993–6997.
43. Tomita S, Li RK, Weisel RD, *et al.* Autologous transplantation of bone marrow cells improves damaged heart function. *Circulation* 1999; **100**: II247–256.
44. Terada N, Hamazaki T, Oka M, *et al.* Bone marrow cells adopt the phenotype of other cells by spontaneous cell fusion. *Nature* 2002; **416**: 542–545.
45. Zhang YM, Hartzell C, Narlow M, Dudley SC Jr. Stem cell-derived cardiomyocytes demonstrate arrhythmic potential. *Circulation* 2002; **106**: 1294–1299.
46. Linask KK, Knudsen KA, Gui YH. N-Cadherin-catenin interaction: necessary component of cardiac cell compartmentalization during early vertebrate heart development. *Dev Biol* 1997; **185**: 148–164.
47. Harigaya K, Handa H. Generation of functional clonal cell lines from human bone marrow stroma. *Proc Natl Acad Sci U S A* 1985; **82**: 3477–3480.

Photon-Modulated Changes of Cell Attachments on Poly(spiropyran-*co*-methyl methacrylate) Membranes

Akon Higuchi,*,† Ayu Hamamura,† Yosuke Shindo,† Hanako Kitamura,† Boo Ok Yoon,† Taisuke Mori,‡ Taro Uyama,‡ and Akihiro Umezawa‡

Department of Applied Chemistry, Seikei University, 3-3-1 Kichijoji Kitamachi, Musashino, Tokyo 180-8633, Japan

Received May 1, 2004; Revised Manuscript Received June 2, 2004

Spiropyran is a photoresponsive molecule, and nonionic spiropyran is reversibly changed by UV irradiation to a hydrophilic polar, zwitterionic merocyanine isomer, and back again by visible light irradiation. A copolymer of nitrobenzospiropyran and methyl methacrylate, poly(NSP-*co*-MMA) was used as a material with a photosensitive surface. UV irradiation of the photosensitive surface of poly(NSP-*co*-MMA)-coated glass plates decreased the water contact angles (11 ± 1°) and increased diameter of a water drop relative to the unexposed surface. Light-induced detachment of platelets and mesenchymal stem (KUSA-A1) cells on poly(NSP-*co*-MMA)-coated glass plates was observed upon simple- and patterned-light irradiation, whereas no light-induced detachment of platelets and mesenchymal stem cells was observed on poly(methyl methacrylate)-coated glass plates. This is a result of the change from a closed nonpolar spiropyran to the polar zwitterionic merocyanine isomer induced by UV irradiation. Light-induced detachment of fibrinogen adsorbed on poly(NSP-*co*-MMA) coated glass plates was also observed in this investigation.

Introduction

In an effort to induce or control surface wetting by liquids, a number of researchers have proposed the use of a variety of means of changing the interfacial properties of materials including electrical potentials and fields,[1,2] temperature,[3,4] light,[5−7] and chemical means.[8] The focus of these studies has been on the manipulation of microchannels, micro-total analysis systems (μ-TAS),[9,10] and the capillary surface using external stimuli. Rosario et al. investigated the microfluidic actuation of water in capillary tubes coated with a photosensitive layer. Water in the capillary tubes was observed to rise on the order of 2.8 mm for a 500 μm diameter capillary, when the wavelength of incident light was switched from the visible region to the UV region. This is thought to be because the relatively nonpolar spiropyran can be reversibly switched to a polar, zwitterionic merocyanine isomer with a much larger dipole moment upon UV light irradiation, and back to the nonpolar spiropyran isomer again upon visible light irradiation.[7]

Surface control of hydrophilic/hydrophobic properties by external stimuli such as temperature change was also reported to develop thermo-responsive culture dishes for cells.[11,12] Hirose and Okano et al. developed designed shape cell sheets for tissue engineering in which human aortic endothelial cells were cultured and proliferated on tissue culture polystyrene dishes grafted with poly(*N*-isopropylacrylamide) (PIPAAm) and poly(*N*,*N*′-dimethylacrylamide) for thermosensitive response of cell adhesive and cell nonadhesive domains.[11] When the culture temperature was reduced below 32 °C (LCST), PIPAAm changed to hydrophilic and the cell sheets detached from PIPAAm-grafted surfaces in the absence of an enzyme such as trypsin.[11]

In this study, we investigated light-induced detachment of platelets and mesenchymal stem (KUSA-A1) cells on poly(NSP-*co*-MMA)-coated glass plates upon simple- and patterned-light irradiation as well as the change of physical properties on the photosensitive surface of poly(NSP-*co*-MMA)-coated glass plates, i.e., hydrophobicity−hydrophilicity change and change of amount of protein adsorption induced by UV irradiation.

Experimental Section

Preparation of Membranes. Poly(NSP-*co*-MMA) was synthesized by a conventional route according to the literature[17,18] and was donated by M. Kameda, K. Sumaru, and T. Kanamori (AIST).[19] Poly(NSP-*co*-MMA), 0.1 wt % in dichloroethane, was cast onto glass plates in flat Petri dishes. PMMA-coated glass plates were also prepared for use as controls.

Physical Characteristic Measurements. The water contact angles of the poly(NSP-*co*-MMA)-coated and PMMA-coated glass plates were measured at 25 °C and 85% relative humidity by the sessile drop method using ultrapure water.[20] The water contact angles were monitored and recorded with a CCD camera (DCR−PC100, Sony Corporation). At least four readings ($n = 4$) were taken at 2 min after placing water droplets (6−7 mm diameter) on different parts of the glass plates, and the values were averaged.

Fibrinogen Adsorption Assay. Fibrinogen adsorption from human plasma on the surface of the poly(NSP-*co*-

* To whom correspondence should be addressed. Tel: +81-422-37-3748. Fax: +81-422-37-3748. E-mail: higuchi@ch.seikei.ac.jp.
† Seikei University.
‡ National Center for Child Health and Development.

10.1021/bm049737x CCC: $27.50
Published on Web 07/07/2004

MMA)-coated and PMMA-coated glass plates was directly evaluated using the method based on the antigen−antibody reaction using enzyme-immunoglobulin conjugate (ELISA assay).[13] Briefly, the poly(NSP-*co*-MMA)-coated and PMMA-coated glass plates were immersed in 50% platelet-poor plasma diluted with phosphate buffer solution (PBS, 0.02M, pH 7.4) containing 0.15 mol/L NaCl for 180 min at 37 °C. After the poly(NSP-*co*-MMA)-coated and PMMA-coated glass plates were rinsed with sufficient PBS and were shifted into another new 24-well tissue culture flask, the poly(NSP-*co*-MMA)-coated and PMMA-coated glass plates were incubated with the primary antibody (i.e., mouse monoclonal anti-human fibrinogen (F4639, Sigma-Aldrich, Inc.)) diluted with Block Ace (UK−B80, Funakoshi Co.) solution for 1 h at 37 °C. Thereafter, the primary antibody was blocked with Block Ace solution after rinsing the glass plates with PBS containing 0.05 wt % Tween 20. The poly(NSP-*co*-MMA)-coated and PMMA-coated glass plates were subsequently incubated with the secondary antibody, rabbit H+L anti-mouse immunoglobulin peroxidase conjugate antibody (014−17611, Wako Pure Chemical Industries, Ltd.) for 60 min at 37 °C.

After sufficiently rinsing the poly(NSP-*co*-MMA)-coated and PMMA-coated glass plates with PBS containing 0.05 wt % Tween 20, 0.6 mL of a H_2O_2 solution containing the substrate for horseradish peroxidase, 3,3′,5,5′-tetramethylbenzidine (TMB Microwell Peroxidase Substrate System, 50−76−00, Kirkegaard & Perry Laboratories), was added to the 24-well tissue culture flask containing the glass plates. The absorbance of the solution was measured at 450 nm after 15 min of the enzyme reaction when the stop solution (1 mole/l H_3PO_4 solution) of the reaction was injected into the 24-well tissue culture flask. These measurements were carried out four times for each glass plates.

Light-Induced Detachment of Platelets. The poly(NSP-*co*-MMA)-coated glass plates in a 24-well tissue culture flask were equilibrated in saline solution at 37 °C for 1 h. The saline solution was removed, and 1 mL of fresh platelet-rich plasma (PRP)[13] was subsequently introduced into each well. The poly(NSP-*co*-MMA)-coated glass plates were incubated with PRP at 37 °C for 30 min. Then, the poly-(NSP-*co*-MMA)-coated glass plates were illuminated with UV irradiation using a handy UV lamp (UVGL-25, 365 nm, 950 μW/cm^2, UVP, Inc.) from the bottom of the 24-well tissue culture flask for 4 min at 37 °C. Control experiments in which the poly(NSP-*co*-MMA)-coated glass plates were not illuminated by UV irradiation were also performed. After 4 min, PRP was removed using a Pasteur pipet and 1 mL of PBS was pipetted into each well of the flask. The platelet numbers on both the poly(NSP-*co*-MMA)-coated glass plates, exposed to UV irradiation and not exposed to UV irradiation, were counted before and after UV irradiation using inverted phase-contrast microscopy (IX70, Olympus Corporation) equipped with a CCD video camera (CS230, Olympus Corporation). Light-induced detachment of platelets on PMMA-coated glass plates was also performed using the same procedures as a control. These measurements were carried out four times for each membrane.

Light-Induced Detachment of KUSA-A1 Cells. Mesenchymal stem cell line, KUSA-A1, derived from the bone marrow of female C3H/He mice (A. U.)[21] was used in this study. The poly(NSP-*co*-MMA)-coated glass plates in the 24-well tissue culture flask were equilibrated with saline solution at 37 °C for 1 h. The saline solution was removed, and 1 mL of KUSA-A1 cell suspension supplemented with DMEM media and 10% fetal bovine serum was subsequently introduced into each well. The poly(NSP-*co*-MMA)-coated glass plates were incubated with KUSA-A1 cells in a constant 5% CO_2 atmosphere at 37 °C for 30 min. Then, the poly(NSP-*co*-MMA)-coated glass plates were illuminated by UV light using the handy UV lamp (UVGL-25, 365 nm, 950 μW/cm^2, UVP, Inc.) from the bottom of the 24-well tissue culture flask for 4 min. When the patterned light irradiation was performed, a striped pattern mask (width; 2.5 mm), made from a transparency sheet (CG3410, 3M), was placed under the well. Additionally, control experiments in which the poly(NSP-*co*-MMA)-coated glass plates were not illuminated by UV irradiation were also performed. After 4 min, the DMEM media was removed using a Pasteur pipet and 1 mL of DMEM media was inserted into each well of the flask. The cell numbers of KUSA-A1 cells on both the poly(NSP-*co*-MMA)-coated glass plates, illuminated and not illuminated by UV irradiation, were counted before and after UV irradiation using inverted phase-contrast microscopy with CCD video camera. Light-induced detachment of KUSA-A1 cells on the PMMA-coated glass plates was also performed as a control according to the same procedure. These measurements were carried out four times for each membrane.

Results and Discussion

Hydrophobicity−Hydrophilicity Change. Hydrophilicity−hydrophobicity change induced by UV irradiation was investigated on poly(NSP-*co*-MMA) (see Figure 1) and poly-(methyl methacrylate) (PMMA) coated glass plates. Figure 2 shows the time dependence of the water contact angle and the diameter ratio (d_t/d_0) of the water drop on poly(NSP-*co*-MMA)-coated and PMMA-coated glass plates where d_0 and d_t are the diameter of water drop at time = 0 and t min after UV (375 nm) irradiation, respectively.

UV irradiation of the control surface of PMMA-coated glass plates demonstrated no change in the water contact angles within the experimental error and only a slight decrease in the diameter of the water droplet. The slight decrease of d_t/d_0 on the PMMA-coated glass plates was attributed to evaporation of water drop during the measurements. The photosensitive surface of poly(NSP-*co*-MMA)-coated glass plates under UV irradiation resulted in decreased water contact angles as well as an increased diameter of water droplet relative to that on the surface before UV light irradiation. The large change in the dipole moment between the two isomeric states of the spiropyran was determined to induce changes in the energy at the surface of poly(NSP-*co*-MMA). Spiropyran-coated photosensitive surfaces were determined to change in the surface energy solely upon light irradiation, as measured by the water contact angle.

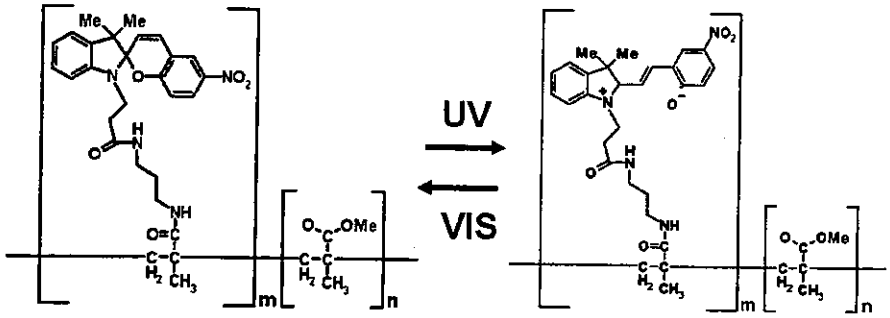

Figure 1. Schematic of transition of poly(NSP-*co*-MMA) upon exposure to UV irradiation.

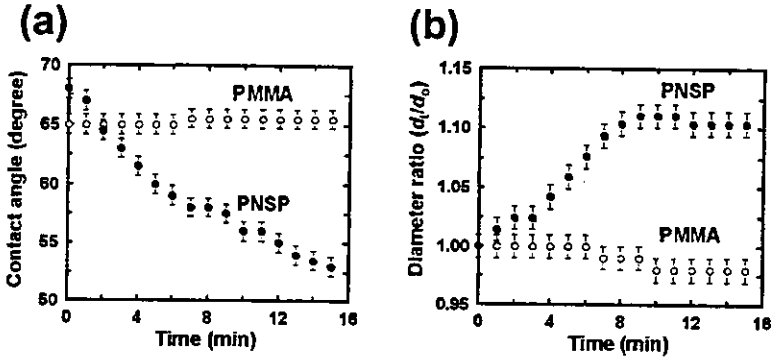

Figure 2. Hydrophobicity–hydrophilicity change on poly(NSP-*co*-MMA)-coated and PMMA-coated glass plates induced by UV irradiation. (a) Time dependence of water contact angle of water drop on poly(NSP-*co*-MMA)-coated and PMMA-coated glass plates. (b) Time dependence of diameter ratio (d/d_0) of water drop on poly(NSP-*co*-MMA) and PMMA coated glass plates. PNSP indicates poly(NSP-*co*-MMA)-coated glass plates.

After the water contact angles on poly(NSP-*co*-MMA)-coated glass plates were measured at first time, the poly-(NSP-*co*-MMA)-coated glass plates were dried under vacuum and in the dark place at ambient temperature for 24 h. After this treatment, the color of poly(NSP-*co*-MMA)-coated glass plates changed from purple color to colorless, which indicated the spiropyran in poly(NSP-*co*-MMA)-coated glass plates returned to the first form of nonionic spiropyran. The water contact angles of the poly(NSP-*co*-MMA)-coated glass plates were again measured. Exactly the same results to Figure 2 were obtained within the experimental error.

Therefore, the reversibility between the form of nonionic spiropyran and that of zwitterionic merocyanine isomer in the poly(NSP-*co*-MMA)-coated glass plates was observed in this study.

Light-Induced Detachment of Cells. Light-induced detachment of platelets and mesenchymal stem (KUSA-A1) cells was also examined. Figure 3 shows KUSA-A1 cells on poly(NSP-*co*-MMA)-coated glass plates before and after UV irradiation. After UV irradiation to the poly(NSP-*co*-MMA)-coated glass plates, KUSA-A1 cells were rarely observed on the surface of poly(NSP-*co*-MMA)-coated glass plates. On the other hand, KUSA-A1 cells remained attached to the surface of poly(NSP-*co*-MMA)-coated glass plates submitted to the same procedures, but not to be exposed to UV irradiation. The cell density of KUSA-A1 cells and platelets on the surface of poly(NSP-*co*-MMA)-coated glass plates before and after UV irradiation was examined and summarized in Figure 4a. In addition, light-induced detachment of KUSA-A1 cells and platelets was examined on

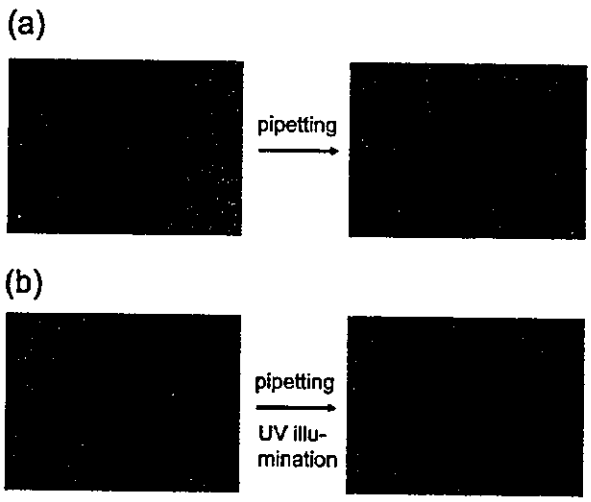

Figure 3. Light-induced detachment of KUSA-A1 cells. (a) KUSA-A1 cells on poly(NSP-*co*-MMA)-coated glass plates. (b) KUSA-A1 cells on PMMA-coated glass plates.

PMMA-coated glass plates, as a nonphotosensitive surface (Figure 4b). Light-induced detachment of KUSA-A1 cells was clearly not observed on PMMA-coated glass plates, indicating that the cell detachment on poly(NSP-*co*-MMA)-coated glass plates upon UV irradiation is not due to the stimulation of the cells by UV light irradiation. Thus, it is thought to be caused by the change in the surface energy and/or the change in the switching movement of closed nonpolar spiropyran to the polar zwitterionic merocyanine isomer upon UV irradiation.

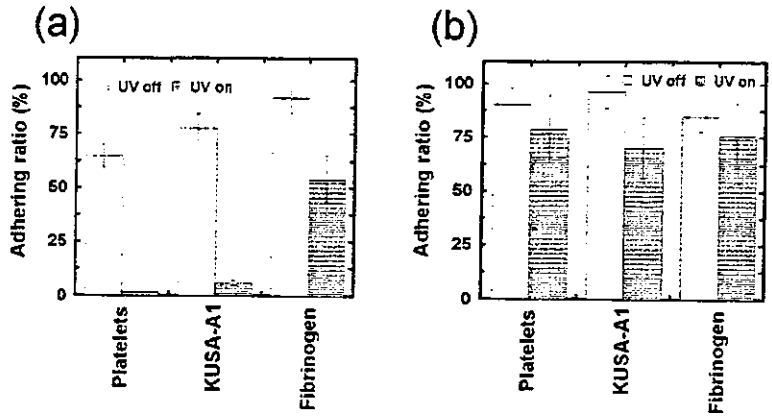

Figure 4. Light-induced detachment of platelets, KUSA-A1 cells and fibrinogen. (a) Platelets, KUSA-A1 cells, and fibrinogen on poly(NSP-*co*-MMA)-coated glass plates. (b) Platelets, KUSA-A1 cells, and fibrinogen on PMMA-coated glass plates.

The cell viability of the detached cells by UV irradiation was found to be more than 98% based on the trypan blue exclusion test.

Light-Induced Detachment of Fibrinogen. Suppression of platelet adhesion is generally believed to be due to a reduction of protein adsorption, particularly fibrinogen, which binds to the platelet membrane glycoprotein GP IIb-IIIa.[13,14] Light-induced detachment of fibrinogen adsorbed on poly(NSP-*co*-MMA) coated glass plates was, therefore, examined (Figure 4a). After the poly(NSP-*co*-MMA) coated glass plates were immersed in platelet-poor plasma (PPP) solution for 30 min, UV light was illuminated on the surface for 4 min, and the fibrinogen adsorbed on the surface was directly measured by an enzyme-immunoglobulin conjugate assay (ELISA).[13] The adsorbed fibrinogen was determined to decrease on the surface of poly(NSP-*co*-MMA)-coated glass plates compared to that on the surface not exposed to UV irradiation.

The following experiments were also performed: The adsorbed amount of fibrinogen was measured on the poly(NSP-*co*-MMA)-coated glass plates where UV light was irradiated for 4 min before the poly(NSP-*co*-MMA)-coated glass plates were immersed into PPP solution (NSP was already in the form of the zwitterionic merocyanine isomer when the poly(NSP-*co*-MMA)-coated glass plates made contact with PPP). The poly(NSP-*co*-MMA) coated glass plates had NSP consisting of zwitterionic merocyanine isomer adsorbed fibrinogen at 6.2 ± 0.5 $\mu g/cm^2$, whereas poly(NSP-*co*-MMA) coated glass plates had NSP consisting of nonionic spiropyran adsorbed at 5.0 ± 0.4 $\mu g/cm^2$. These findings indicate that the amount of adsorbed fibrinogen on the glass plates with the zwitterionic merocyanine isomer NSP was 1.2 times higher than that with the nonionic spiropyran NSP. These finding were not in agreement with the results shown in Figure 4a. This contradiction suggests that the fibrinogen was detached by means of the switching movement of closed nonpolar spiropyran to the polar zwitterionic merocyanine isomer, and the surface energy (hydrophobicity−hydrophilicity) does not directly contribute to the amount of adsorbed fibrinogen on the poly(NSP-*co*-MMA) coated glass plates. Light-induced detachment of fibrinogen was also examined on the PMMA-coated glass plates, as a nonphotosensitive surface and is shown in Figure 4b. No light-induced detachment of fibrinogen was observed on the PMMA-coated glass plates. This further indicates that fibrinogen detachment by UV irradiation is not due to the stimulation of fibrinogen by UV light, but a result of the change in the switching movement of closed nonpolar spiropyran to the polar zwitterionic merocyanine isomer upon UV irradiation.

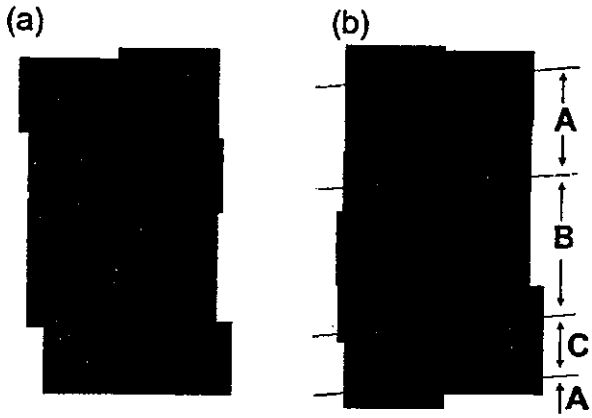

Figure 5. Light-induced detachment of KUSA-A1 cells with patterned light irradiation using striped pattern mask with 2.5 mm widths. (a) KUSA-A1 cells on poly(NSP-*co*-MMA)-coated glass plates before UV irradiation. (b) KUSA-A1 cells on poly(NSP-*co*-MMA)-coated glass plates after striped pattern UV irradiation for 4 min. Regions A and B indicate the area under non-UV irradiation (region A) and UV irradiation (region B), respectively. Region C indicates the border region.

Cell Detachment by Patterned Light Irradiation. Light-induced detachment of KUSA-A1 cells was achieved by simple patterned light irradiation using a striped pattern mask (width; 2.5 mm). Figure 5 shows KUSA-A1 cells on poly(NSP-*co*-MMA)-coated glass plates before and after UV irradiation with the striped pattern. KUSA-A1 cells were clearly observed to detach in the region exposed to UV irradiation (region B), whereas the cells remained attached in the masked area, not exposed to UV irradiation (region A). Therefore, patterned light detachment of KUSA-A1 cells was successively performed by the patterned light irradiation using the striped pattern mask.

Conclusion

KUSA-A1 cells, platelets, and the fibrinogen were detached by means of the switching movement of closed nonpolar spiropyran to the polar zwitterionic merocyanine isomer, and the surface energy (hydrophobicity−hydrophilicity) does not directly contribute to the amount of adsorbed fibrinogen on the poly(NSP-*co*-MMA)-coated glass plates.

Light-induced detachment of cells on poly(NSP-*co*-MMA) surfaces will lead to mild isolation of cells. Furthermore, this will be a powerful tool for surface marker analysis using flow cytometry. This is because this method does not require the addition of trypsin for cell detachment, which degrades the extracellular matrix and cell adhering molecules between cells and the culture flask. Furthermore, patterned light detachment of nerve cells will provide an alternative method to create micro-patterned neuronal networks,[15] which are typically performed using a micro-contact printing method.[16]

Acknowledgment. We thank Dr. M. Kameda, Dr. K. Sumaru, and Dr. T. Kanamori (AIST) for their gift of poly(NSP-*co*-MMA). This research was partially supported from a Grant-in-Aid for Exploratory Research (No. 14655136) from the Ministry of Education, Culture, Sports, Science, and Technology of Japan. This research was also supported from Asahi Glass Foundation.

References and Notes

(1) Lee, H. J.; Fermin, D. J.; Corn, R. M. *Electrochem. Commun.* **1998**, *1*, 190.
(2) Digilov, R. *Langmuir* **2000**, *16*, 6719.
(3) Liang, L.; Shi, M.; Viswanathan, V. V.; Peurrung, L. M.; Young, J. S. *J. Membr. Sci.* **2000**, *177*, 97.
(4) Yakushiji, T.; Sakai, K.; Kikuchi, A.; Aoyagi, T.; Sakurai Y.; Okano T. *Langmuir* **1998**, *14*, 4657.
(5) Garcia, A. A.; Cherian, S.; Park, J.; Gust, D.; Jahnle, F.; Rosario, R. *J. Phys. Chem. A* **2000**, *104*, 6103.
(6) Ichimura, K.; Oh, S.; Nakagawa, M. *Science* **2000**, *288*, 1624.
(7) Rosario, R.; Gust, D.; Hayes, M.; Jahnke, F.; Springer, J.; Garcia, A. A. *Langmuir* **2002**, *18*, 8062.
(8) Lee, S.; Laibinis, P. E. *J. Am. Chem. Soc.* **2000**, *122*, 5395.
(9) Vo-Dinh, T.; Alarie, J. P.; Isola, N.; Landis, D.; Wintenberg, A. L.; Ericson, M. N. *Anal. Chem.* **1999**, *71*, 358.
(10) Maims, C.; Hulme, J.; Fielden, P. R.; Goddard, N. J. *Actuator B, Chem.* **2001**, *77*, 671.
(11) Hirose, M.; Kwon, O. H.; Yamato, M.; Kikuchi, A.; Okano, T. *Biomacromolecules* **2000**, *1*, 377.
(12) Ratner, B. R.; Horbett, T.; Hoffman, A. S.; Hauschka, S. D. *J. Biomed. Mater. Res.* **1975**, *9*, 407.
(13) Higuchi, A.; K. Sugiyama, K.; Yoon, B. O.; Sakurai, M.; Hara, M.; Sumita, M.; Sugahara, S.; Shirai, T. *Biomaterials* **2003**, *24*, 3235.
(14) Phillips, D. R.; Charo, I. F.; Parise, L. V.; Fitzgerald, L. A. *Blood* **1988**, *71*, 831.
(15) Higuchi, A.; Kitamura, H.; Shishimine, K.; Konishi, S.; Yoon, B. O.; Hara, M. *J. Biomat. Sci., Polym. Ed.* **2003**, *14*, 1377.
(16) Kam, L.; Shain, W.; J. N. Turner, J. N.; Bizios, R. *Biomaterials* **2001**, *22*. 1049.
(17) Imai, Y.; Adachi, K.; Naka, K.; Chujo Y. *Polym. Bull.* **2000**, *44*, 9.
(18) Labsky J.; Koropecky, I.; Nespurek, S.; Katal, J. *Polym. J.* **1981**, *17*, 309.
(19) Kameda, M.; Sumaru, K.; Kanamori, T. in preparation.
(20) Higuchi, A.; Tamiya, S.; Tsubomura, T.; Katoh, A.; Cho, C. S.; Akaike, T.; Hara, M. *J. Biomater. Sci. Polymer Ed.* **2000**, *11*, 149.
(21) Umezawa, A.; Maruyama, T.; Segawa, K.; Shadduck, R. K.; Waheed, A.; Hata, J. *J. Cell. Physiol.* **1992**, *151*, 197.

BM049737X

Modern Pathology (2004) 17, 423–429

www.modernpathology.org

Diagnostic importance of CD179a/b as markers of precursor B-cell lymphoblastic lymphoma

Nobutaka Kiyokawa[1], Takaomi Sekino[1], Tsubasa Matsui[1], Hisami Takenouchi[1], Kenichi Mimori[1], Wei-ran Tang[1], Jun Matsui[1], Tomoko Taguchi[1], Yohko U Katagiri[1], Hajime Okita[1], Yoshinobu Matsuo[2], Hajime Karasuyama[3] and Junichiro Fujimoto[1]

[1]*Department of Developmental Biology, National Research Institute for Child Health and Development, Japan;* [2]*Fujisaki Cell Center, Hayashibara Biochemical Labs Inc, Okayama, Japan and* [3]*Department of Immune Regulation, Tokyo Medical and Dental University, Graduate School of Medicine, Tokyo, Japan*

Surrogate light chains consisting of VpreB (CD179a) and λ5 (CD179b) are expressed in precursor B cells lacking a complete form of immunoglobulin and are thought to act as substitutes for conventional light chains. Upon differentiation to immature and mature B cells, CD179a/b disappear and are replaced with conventional light chains. Thus, these molecules may be useful as essential markers of precursor B cells. To examine the expression of the surrogate light-chain components CD179a and CD179b in precursor B-cell lymphoblastic lymphoma, we analyzed tissue sections using immunohistochemistry techniques. Among a number of monoclonal antibodies for the surrogate light chains, VpreB8 and SL11 were found to detect CD179a and CD179b, respectively, in acetone-fixed fresh frozen sections. Moreover, we also observed VpreB8 staining in formalin-fixed, paraffin-embedded sections. Using these antibodies, we found that CD179a/b were specifically expressed in precursor B-cell lymphoblastic lymphomas, but not in mature B-cell lymphomas in childhood. Furthermore, other pediatric tumors that must be included in a differential diagnosis of precursor B-cell lymphoblastic lymphoma, including precursor T-cell lymphoblastic lymphoma, extramedullary myeloid tumors, and Ewing sarcoma, were also negative for both CD179a and CD179b. Our data indicate that CD179a and CD179b may be important markers for the immunophenotypic diagnosis of precursor B-cell lymphoblastic lymphomas.
Modern Pathology (2004) **17,** 423–429, advance online publication, 20 February 2004; doi:10.1038/modpathol.3800079

Keywords: CD179a/b; lymphoblastic lymphoma; precursor B cells; immunohistochemistry; diagnosis

B cells are characterized by the surface expression of immunoglobulin (Ig), consisting of a heavy chain (HC) and conventional κ or λ light chains (LCs). The Ig expressed in B cells is associated with the Igα/Igβ (CD79a/b) complex and forms a B-cell antigen receptor complex. In contrast to these mature B cells, precursor B cells do not express Ig, although they do contain Ig-related components. For example, more primitive pro-B cells already express the Igα/Igβ complex and contain surrogate LCs, consisting of VpreB (CD179a) and λ5 (CD179b).[1–5] Through the successful rearrangement of HC genes, pro-B cells undergo differentiation into pre-B cells and start to express a premature antigen receptor, namely the pre-B-cell receptor (pre-BCR), consisting of μ HC, CD179a/b and the Igα/Igβ heterodimer.[6–9] Upon further differentiation from pre-B cells to B cells, CD179a/b disappear and are replaced with conventional LC.

The stage-specific developmental expression of Ig-related molecules is an essential characteristic of B-lineage cells and is conserved not only in normal cells but also in neoplastic cells of B lineage. Indeed, precursor B acute lymphoblastic leukemias (ALL), which originate from precursor B cells and lack the complete form of Ig, are known to express CD179a/b, while mature and Ig-expressing B-cell ALLs do not.[10] Precursor B-cell lymphoblastic lymphoma (B-LBL) is a disease in which neoplastic precursor B cells proliferate without the obvious involvement of blood or bone marrow and thus exhibits immunophenotypic characteristics that are similar to those of precursor B-ALL.[11,12] Neoplasms of precursor B cells most commonly present as a form of ALL during childhood, and the presentation of B-LBL is infrequent, but may occur in patients of any

Correspondence: N Kiyokawa, MD, PhD, Department of Developmental Biology, National Research Institute for Child Health and Development, 3-35-31, Taishido, Setagaya-ku, Tokyo 154-8567, Japan.
E-mail: nkiyokawa@nch.go.jp
Received 21 August 2003; revised 26 November 2003; accepted 26 December 2003; published online 20 February 2004

age, frequently involving the skin, bone, or lymph nodes. Owing to the rareness of B-LBL and its morphological and immunophenotypic similarities to mature B-cell lymphomas in some cases, distinguishing between these diseases is of great importance, especially in the field of pediatric oncology, because the treatment strategies for these two diseases are quite different. In addition, other tumors, including precursor T-cell lymphoblastic lymphoma (T-LBL), extramedullary myeloid tumors, and Ewing sarcoma, must also be included in a differential diagnosis of B-LBL.

In an attempt to characterize B-LBL using the expression of Ig-related molecules and to examine the utility of such a method for diagnosis, we examined CD179a/b expression in B-LBL tissues using immunohistochemistry. CD179a/b was found to be specifically expressed in B-LBL, but not in mature B-cell lymphomas and other tumors in childhood. The usefulness of CD179a/b as diagnostic markers for B-LBL is discussed.

Materials and methods

Materials

The human pre-B-cell line HPB-NULL[10] and the Burkitt cell line Ramos (Japanese Cancer Research Resources Bank, Tokyo, Japan) were used in this study. Cells were maintained in RPMI1640 supplemented with 10% fetal calf serum at 37°C in a humidified 5% CO_2 atmosphere.

Biopsy specimens from pediatric patients, including 11 patients with B-LBL, seven patients with Burkitt lymphoma, three patients with diffuse large B-cell lymphoma, seven patients with T-LBL, three patients with extramedullary myeloid tumors, and three patients with Ewing sarcoma, were selected from medical files collected between 1985 and 2003 at the Department of Developmental Biology, National Research Institute for Child Health and Development. In each case, the initial diagnosis was based on morphological observations of hematoxylin and eosin (H&E)-stained, formalin-fixed, paraffin-embedded tissues, the immunophenotypic characteristics revealed by immunohistochemistry using acetone-fixed, fresh frozen sections, and the patient's clinical features. In some cases, immunophenotyping was also performed using flow cytometric analysis of a single-cell suspension prepared from the tissue. To examine CD179a/b expression, snap-frozen tissues in OCT compounds stored at −85°C after the initial diagnosis were used.

The following mouse monoclonal antibodies (mAbs) were used in this study: anti-CD179a (HSL96), anti-CD179b (HSL11), anti-conformational pre-BCR (HSL2),[10] anti-CD20 (L26),[13] anti-HLA-DR,[14] and anti-CD10 (IF6).[15] HSL2 is a unique mAb that does not bind to each component of the pre-BCR, but recognizes a conformational epitope formed only when the μ HC and CD179a/b surrogate LC associate with each other to make the pre-BCR complex.[10] In addition, several commercially available mAbs were also used: anti-μ (G20-127), anti-CD179a (VpreB8 and VpreB9), and anti-CD19 (Leu12) from BD Pharmingen (San Diego, CA, USA); anti-κ (HP6053) and anti-λ (HP6054) from Zymed Laboratories Inc. (San Francisco, CA, USA); anti-CD79a (HM-57), anti-CD22 (4KB128), and anti-TdT (HT-1/3/4) from DAKO (Glostrup, Denmark); anti-CD179a (4G7) from Coulter/Immunotech Inc. (Westbrook, MA, USA); anti-TdT (SEN28) from Nichirei Co. (Tokyo, Japan); and anti-CD179a (B-MAD-688) from Biocarta (San Diego, CA, USA). The anti-CD77 (1A4) used in this study was a generous gift from Dr S Hakomori of the University of Washington, Seattle, WA, USA and Otsuka Assay Laboratories, Kawauchi-cho, Tokushima, Japan. Secondary Abs, including fluorescence- and enzyme-conjugated Abs, were purchased from Jackson Laboratory, Inc., West Grove, PA, USA.

Flow Cytometry

The cells were stained with mAbs and analyzed by flow cytometry (EPICS-XL, Coulter) as described previously.[15] Cytoplasmic antigens were stained using CytoStain™ Kits (BD Pharmingen), according to the manufacturer's protocol.

Immunohistochemistry

Immunohistochemical staining of acetone-fixed fresh frozen sections was performed as described elsewhere.[16] Briefly, fresh frozen sections from each tissue were prepared using a cryostat apparatus and fixed in acetone for 15 min at 4°C. After washing in phosphate-buffered saline (PBS) and blocking with normal rabbit serum, the sections were incubated with mAbs at appropriate dilutions for 30 min at room temperature. Sections were then washed with PBS and incubated with horseradish peroxidase (HRP)-conjugated rabbit anti-mouse antibodies for 30 min at room temperature. After washing with PBS, color development was performed in diaminobenzidine solution (10 mM in 0.05 M Tris-HCl, pH 7.5) with 0.003% H_2O_2.

For the cell line samples, the cells were cytocentrifuged on slide glasses using Cytospin III (Shandon Scientific Ltd., Pittsburgh, PA, USA). After fixation with acetone, immunohistochemical staining was performed as described above. In addition, other fixatives, including paraformaldehyde and Zamboni's fixative, were also tested.

The formalin-fixed, paraffin-embedded tissue specimens were initially deparaffinized and then treated using the heat-induced epitope retrieval method in 10 mM of citrate buffer, pH 6.0; immunohistochemical staining was performed using the CSA system (DAKO) according to the manufacturer's protocol.

Results

Immunohistochemical Staining of CD179a/b in Acetone-fixed Cytocentrifuged Cell Lines

As reported previously and presented in Figure 1, the mAbs HSL96, HSL11, and HSL2 recognized CD179a/VpreB, CD179b/λ5, and conformational pre-BCR, respectively, in membrane-permeabilized cells when analyzed using flow cytometry.[10] We first examined whether these mAbs could also be used for immunohistochemical staining in acetone-fixed cells. When acetone-fixed, cytocentrifuged pre-B-ALL HPB-NULL cells expressing conformational pre-BCR were tested, the HSL11 mAb was able to detect CD179b at a concentration of 5 μg/ml; neither the HSL96 nor the HSL2 mAbs detected this molecule (Figure 1). Typically, a cytoplasmic staining pattern was observed in HPB-NULL cells using HSL11. In contrast, HSL11 did not react with similarly treated Ramos Burkitt cells, which express the complete form of Ig (μλ), but lack the surrogate LCs, suggesting that CD179b binds specifically to SL11.

We also examined the staining patterns produced by commercially available anti-CD179a mAbs: VpreB8, VpreB9, 4G7, and B-MAD-688. When these four anti-CD179a mAbs were examined, only the VpreB8 mAb reacted with CD179a in acetone-fixed HPB-NULL cells (data not shown). However, VpreB8 mAb exhibited a weak nonspecific binding with the nuclei of acetone-fixed Ramos cells at high mAb concentrations. A concentration of 1.25 μg/ml was optimized as a sufficient and specific condition for CD179a detection in precursor B-ALL cells, which does not produce a nonspecific reaction in Burkitt cells (data not shown).

We further examined whether SL11 and VpreB8 could be used for immunohistochemical staining in cells treated with other fixatives and observed that both mAbs react with Zamboni's fixative-treated cells, but not with paraformaldehyde-treated cells (data not shown).

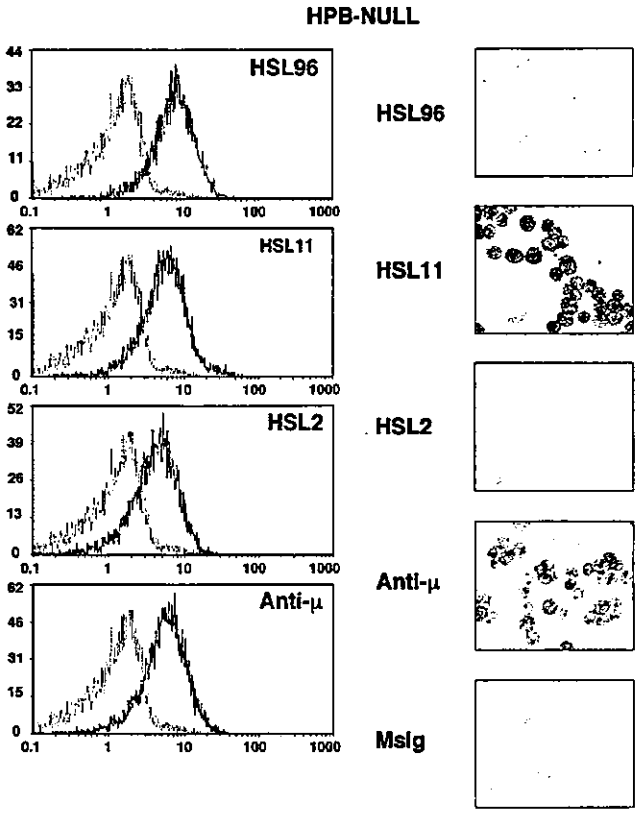

Figure 1 Immunohistochemical detection of CD179b by HSL11 in acetone-fixed, cytocentrifuged precursor B-ALL cell lines. Pre-BCR-expressing HPB-NULL cells were permeabilized and stained with specific mAbs, as indicated, and analyzed using flow cytometry (left panels). The resulting histograms (solid lines) were superimposed on those of the negative control (cells stained with isotype-matched control mouse Ig, broken light lines) and displayed. *X*-axis, fluorescence intensity; *Y*-axis, relative cell number. In parallel, HPB-NULL cells were cytocentrifuged, acetone-fixed, and stained with each mAb, as indicated, using immunohistostaining (right panels). HSL11 is strongly positive and anti-μ is moderately positive, but others are negative. MsIg, iso-type matched control mouse immunoglobulin.

Immunohistochemical Staining of CD179a/b in Acetone-fixed Fresh Frozen Tissues

Next, we used immunohistochemistry to examine whether VpreB8 and HSL11 could detect CD179a/b in clinical childhood B-LBL specimens. When acetone-fixed fresh frozen sections prepared from biopsy specimens obtained from B-LBL patients were examined using immunohistochemical staining, both VpreB8 and HSL11 were found to react with the tissues (Figure 2 and Table 1). Typically, a diffuse cytoplasmic staining pattern was observed in B-LBL tissues using both mAbs (Figure 2). Cases were considered as positive if most of the blasts present in the tissue were clearly stained. As summarized in Table 1, nine out of 10 (90%) B-LBL patients and eight out of 11 (73%) B-LBL patients were positive for VpreB8 and HSL11, respectively. In contrast, no positive staining for VpreB8 or HSL11 was seen in either the Burkitt lymphoma tissues (seven cases) or the diffuse large B-cell lymphoma tissues (three cases), suggesting that both VpreB8 and HSL11 react specifically with B-LBL cells, but not with mature B-cell lymphomas in childhood.

We also examined the other pediatric tumors that must also be included in a differential diagnosis of B-LBL. As presented in Table 2, when acetone-fixed fresh frozen sections prepared from biopsy specimens obtained from seven T-LBL cases, three extramedullary myeloid tumors, and two Ewing sarcoma cases were examined similarly, all of these cases were negative for both VpreB8 and HSL11, indicating the specificity of these mAbs to B-LBL cells.